LUND
UNIVERSITY

Time-resolved study of charge photo-generation in polymer-based solar cells with low driving force

Paulius Baronas

Paulius.Baron@gmail.com

June 10, 2014

Master's thesis work carried out at

The Department of Chemical Physics. Lund University.

Supervisor: Arkady Yartsev, arkady.yartsev@chemphys.lu.se

Examiner: Claudio Verdozzi, claudio.verdozzi@teorfys.lu.se

Abstract

Organic polymer-based solar cells recently attracted much attention as an efficient and inexpensive light-to-electricity conversion solution. However, the mechanism behind charge generation processes in organic materials is still not fully understood due to complex nature of carbon-based compounds. Studies of charge generation, recombination and transport processes are essential for revealing the critical power conversion efficiency (PCE) limiting factors. In this thesis, polymer and fullerene bulk heterojunction (BHJ) solar cells are addressed. In particular, charge generation processes were investigated as a function of driving force in two polymer-fullerene systems. The time resolved photoluminescence (TRPL) studies allowed to investigate ultrafast processes occurring within the timescale of picoseconds. Clear evidence of fast excitation diffusion process (~10ps) was found in pure polymer materials, allowing an assumption that most excitons may reach the interface in polymer-fullerene blends. A strong correlation between higher driving force and photocurrent was shown for polymer based solar cells. The driving force of 0.1 eV for P3TI was proven to be sufficient to dissociate polymer excitons, which indicates a surprisingly low exciton binding energy. In combination with faster exciton diffusion, this suggests the P3TI has superior properties for charge generation compared to similar PTI-1 polymer. Further analysis was focussed on investigation of possible “hot” exciton and charge-transfer (CT) state dissociation.

Keywords:

Organic polymer solar cells, BHJ solar cells, Charge photo-generation, Driving force, Time resolved photoluminescence, CT states.

Abbreviations and acronyms

BHJ	Bulk hetero-junction
BR	Bimolecular recombination
CS	Charge separation
CT	charge transfer
DIO	1,8-octanedithiol (OT) or 1,8-diiodooctane
EET	Excitation energy transfer
GR	Geminate recombination
HOMO	highest occupied molecular orbital
IC	internal conversion
ISC	intersystem crossing
ITO	indium tin oxide
LUMO	lowest unoccupied molecular orbital
MIM	metal-insulator-metal
MO	molecular orbital
OD	optical denisty
P3TI	poly[6,6'-Bis(5'-bromo-3,4'-dioctyl-[2,2'-bithiophen]-5-yl)-1,1'-bis(2-hexyldecyl)-[3,3'-biindolinylidene]-2,2'-dione]
$PC_{61}BM$	[6,6]phenyl-C_{61}-butyric acid methyl ester
$PC_{71}BM$	[6,6]-phenyl-C_{71}-butyric acid methyl ester
PEDOT:PSS	poly(3,4-ethylenedioxythiophene): poly(styrenesulfonate)
PES	potential energy surface
PFPA-1	poly(3,3′-([(9′,9′-dioctyl-9H,9′H-[2,2′-bifluorene]-9,9-diyl)bis(4,1 phenylene)] bis(oxy))bis(N,N-dimethylpropan-1-amine)
PTI-1	poly[N,N′-bis(2-hexyldecyl)isoindigo-6,6′ diyl-alt-thiophene-2,5-diyl]
TRPL	Time-resolved photoluminescence
VR	vibrational relaxation

Contents

1 Introduction

Growing population and development of new technology in the past century have created a demand for large scale energy production. Economic reasons as well as lack of scientific knowledge lead to straightforward solution – generating large amounts of electricity in fossil fuel burning power plants. These days, notwithstanding the decelerating growth of consumption the energy is still produced from fossil fuel burning energy sources that cause environmental hazards such as release of green-house gasses. Inability to solve global environmental issues provides a substantial motivation for development of alternative energy sources. Conversion of solar energy into electricity is the most promising field of renewable energetics since it has a potential capacity of providing thousand times of the world's current energy demand. The cumulative global photovoltaic energy production in 2012 was estimated to be 110 TWh, which contributed to 2.6% of the electricity demand in Europe[1]. However, the costly and complicated manufacturing process remains the major factor limiting the potential of photovoltaic. The average sum of installation and maintenance cost of 0.7 $/W amounts to double the price of fossil fuel generation[2]. Nevertheless, the increasing demand for clean electricity initiated the development of new generation solar cells that are based on organic materials. Compared to conventional inorganic semiconductor based solar cells, the novel technology would offer several advantages, such as flexibility of the device and ease of manufacturing [3]. The experience in plastic material processing would allow the low cost and large scale production of polymer-based solar cells. The current achievements of up to 10% power conversion efficiency attracted first investments leading to commercial applications. However, the general efficiency of the organic photovoltaics is still insufficient compared to their silicon based counterparts. Therefore, the main task of research remains to acquire better understanding of the physical principles of photon-to-current conversion in organic materials.

1.1 Aim and outline of the thesis

Early demonstrations of photon-to-current generation in organic materials attracted significant interest of the scientific community since carbon-based compounds were previously assumed to be incapable of conducting electrical current. Following researches have found that mechanism for solar cell operation cannot be fully described by conventional semiconductor theory. Since then a number of different models was developed to account for charge generation and transport processes in organic materials. Currently, some of the important current generation principles are still actively debated. This allows to assume that further development of new materials and design concepts would lead to significant increase in organic solar cell efficiency.

At the moment, one of the most promising concepts of organic solar cells is based on charge generation in bulk hetero junction (BHJ), which is a blend of conjugated polymer (as electron donor) and fullerene (electron acceptor) systems. The polymer here is used as a light harvester, for its pronounced light absorption capabilities, and the polymer-fullerene interface provides an additional energy (offset between donor and acceptor LUMO levels) for charge formation via charge transfer between donor and acceptor. In common practice this energy is referred to as driving force for charge transfer [4]. Normally, in order to efficiently dissociate polymer excitons, the minimum driving force

of 0,3 eV is required, however recent researches indicated that low offset (~0.1 eV) is sufficient to efficiently generate charges[5]. Due to heterogeneous properties of the polymer and fullerene mix, the energy transfer process in the polymer phase plays an important role in delivering the primary excitation energy to the interface. Extensive studies identified relatively efficient charge photo-generation, separation and transport processes in BHJ, which lead to formulation of several possible physical models of these processes [6], [7]. One of them is based on formation of an intermediate charge-transfer (CT) state, which is essential in the process of generating electron and hole pairs and hence is strongly related to the open circuit voltage of a solar cell [8]. However, the dynamics of the CT state is still not fully understood and requires an investigation utilizing time resolved techniques.

This thesis is focused on a thorough investigation of the photo-physical processes in polymer-fullerene solar cells by means of time resolved photoluminescence techniques. In particular, the efficiency of processes in the solar cell was studied as the function of low driving force. Previous characterization of the solar cells performed by Prof. Inganäs' group from Linkoping University (**Table 1**) confirmed that the current generation is present in all material blend systems. However, the resulting overall efficiency of the solar cell differed significantly. The study of ultrafast charge generation has helped to evaluate the contribution of specific material properties to the final device performance. Additionally, the collected information allowed to speculate on several controversial models for charge gerneration in organic materials, which are currently intensively discussed by scientific community.

Table 1. Electrical properties of solar cells produced with different polymer:fullerene blends. External quantum efficiencies (EQE) provided information about charge generation in different materials.

Sample	j_{sc} (mA/cm^2)	FF	V_{oc}(V)	EQE (%)
PTI-1:PC$_{61}$BM 2:3 2.5%DIO	1,42	0,48	0,918	0,626
PTI-1:PC$_{71}$BM 1:2 2.5%DIO	1,895	0,4	0,884	0,67
P3TI:PC$_{71}$BM 2:3 2.5%DIO	8,241	0,496	0,691	2,825

j_{sc} – short circuit current
FF – fill factor
V_{oc} – open circuit voltage
EQE – external quantum efficiency

2 Organic solar cells

In a conventional semiconductor based device, the process of charge generation can be described using a simplified energy-band model. The light absorption results in excitation of relatively free electrons and holes in a conduction and valence bands. However, this simplistic picture cannot entirely account for the charge generation processes in the active layers of organic materials. The lack of a three-dimensional crystal lattice, different intramolecular and intermolecular interactions, structural disorders and impurities, all result in complex band structure of organic compounds[9]. Therefore, a more detailed model of discrete energy levels is usually considered to describe the processes in conjugated organic materials.

This chapter will first provide a general overview on the nature of electronic states in organic molecules and their interaction with light. Later, the origin of charge generation processes in the conjugated polymers will be described.

2.1 Electronic states in organic molecules

The majority of organic compounds exhibit insulating properties due to the lack of free valence band electrons. However, the conduction of a relatively free charge in organic molecules can be achieved by formation of conjugated systems. Connection of Carbon atoms with alternating double and single bonds results in sp^2 hybridization and hence one out of four outer shell carbon electrons is not involved in formation of strong σ-bonds. An electron which is not localized in σ-bonds, creates a p-orbital, and system of overlapping p-orbitals is connected with π-bonds as it is shown in Figure 2.1 (a). Therefore, electrons become delocalized throughout the whole conjugated system of the molecule.

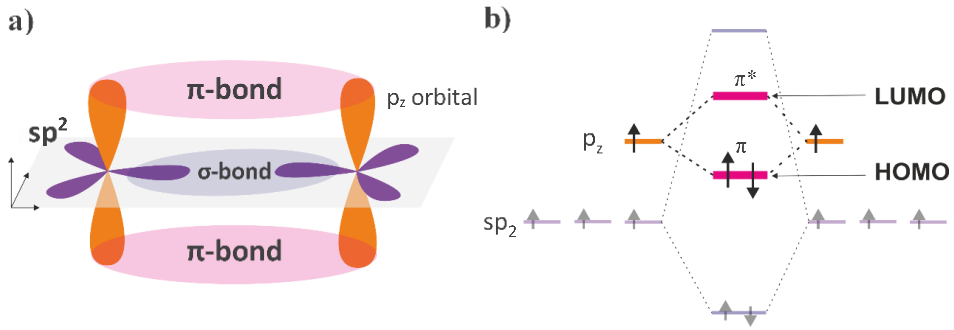

Figure 2.1. The graphical illustration of p-orbitals between two sp^2 hybridization atoms (a) and the representation of energetical distribution of molecular orbitals (b). LUMO and HOMO levels are indicated.

The electronic states of the molecule correspond to specific electron distribution in the molecular orbitals. The π-bonds consist of bonding (π) and antibonding (π*) molecular orbitals that correspond to the lowest unoccupied molecular orbital (LUMO) and the highest occupied molecular orbital

(HOMO), respectively (Figure 2.1 (b)). The electronic excitation of a molecule could be described as an electron transition from HOMO to LUMO molecular orbitals. This transition can be considered as an electron jump from valence to conduction band in conventional semiconductor theory. Therefore, the energy band gap (E_g) is defined as the energy difference between HOMO and LUMO levels. The band gap energies for organic compounds are in the range of 1-4 eV. One of the intrinsic properties of the organic semiconductors is the ability to tune the electronic properties of the system by modifying the molecular structure of the material. Therefore, light absorption, charge generation and transport properties can be optimized for specific requirements.

2.2 Conjugated polymer based solar cells

The discovery of conductive properties in conjugated polymers in 1977 by Shirakawa, Heeger and McDimiarmid was awarded by Nobels prize in 2000 and initiated the development of polymer based electronics[10]. The most interesting property of conjugated polymers was the ability to alter their conductivity in the wide range, which is achieved by doping with inorganic compounds. Electrical conductivity together with superior light absorption properties triggered the major research for employing conjugated polymers in the solar cells as an active layer.

The first solar cells were based on a monolayer structure, where polymer was sandwiched between two different work function electrodes. However, this resulted in very low power conversion efficiency (<1%). The main reason for inefficient charge generation processes is the intrinsic property of organic conjugated compounds. Absorption of light leads to formation of a neutral excited state, called an exciton, which is simply a bound state of electron and corresponding hole. Typically, exciton binding values in organic materials are high, therefore, some additional energy is required to drive charge separation. The breakthrough in the organic solar cell science was achieved by introducing the double layered structures. The bilayer system consist of electron donor and electron acceptor molecular materials. The exciton is created in donor material (usually conjugated polymer) and later diffuses to the interface of the layers. There, the potential energy difference (caused by acceptors larger electron affinity) initiates dissociation of the exciton into free charges. Nonetheless, the majority of excitons are generated at the top of polymer layer (due to high absorption coefficient) and hence never reach the interface because of the limited diffusion length (~10 nm). The limitations induced by absorption, exciton diffusion and layer thickness can be overcome by adapting the right layer morphology. This idea lead to the development of a bulk heterojunction solar cell (BHJ) concept, where instead of layering donor and acceptor, a fine mixture of materials was introduced in a single layer structure (

Figure **2.2**). The significantly increased solar cell performance suggesting that due to the reduced diffusion its path for the exciton, the dissociation into charges is a more efficient process. Even further increase of power generation was observed by improving percolation pathways for charges to be transported to the electrodes more efficiently[11]. The best bulk hetero junction solar cells currently reached power conversion efficiency of up to 10%[12].

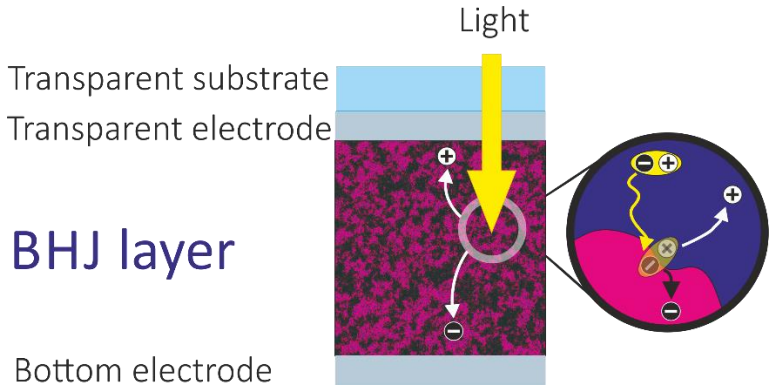

Figure 2.2. Scheme and operational principle of the bulk heterojunction solar cell.

Considering the materials, BHJ solar cells are usually based on using polymer as a donor and fullerene as an electron acceptor. Fullerene derivatives [6,6]-Phenyl-C_{61}-butyric acid methyl ester (**$PC_{61}BM$**) and [6,6]-phenyl-C_{71}-butyric acid methyl ester (**$PC_{71}BM$**) have been the most widely used acceptors in BHJ systems[9], [13]. In contrast, the variety of donor material is relatively broad, since the properties of absorption, exciton diffusion and charge transport have to be taken into consideration. A common design of low band gap polymers is to combine electron-rich (donor) and electron-deficient (acceptor) groups as repeating units, forming internal donor–acceptor (D–A) structures[14]. In this thesis, two low band gap isoindigo-based polymer systems (Figure 2.3) were investigated, in order to study the effects of driving force in BHJ blends. **PTI-1** polymer consist of alternating electron-rich thiophene as the donor and isoindigo as the acceptor[15]. In **P3TI** structure, the thiophene unit is changed to terthiophene, which is thought to be a more promising donor unit since it employs more planar structure and thus beneficial for increasing polymer conjugation[16].

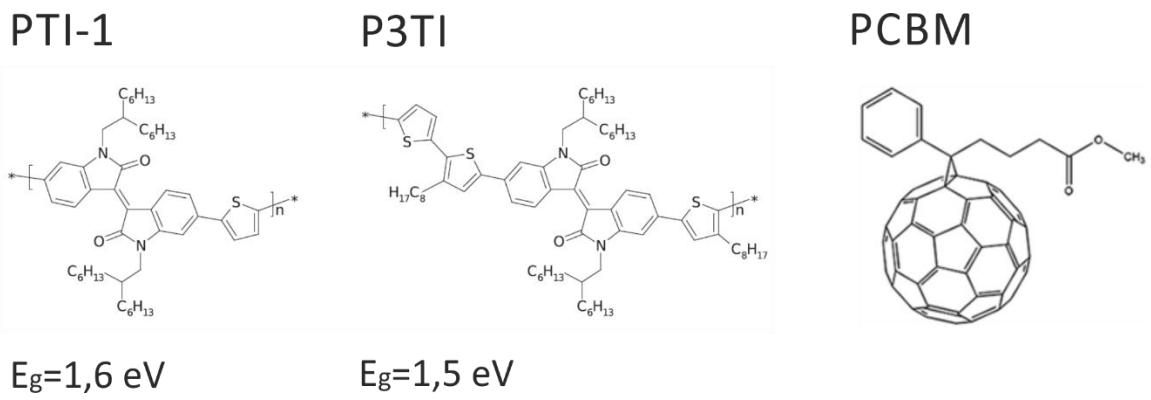

Figure 2.3. The molecular structure of conjugated polymers (PTI-1 and P3TI) and fullerene derivative (PCBM). Effective band gaps of the polymers are indicated.

The solar cells were produced by depositing the active material layers on top of the glass substrate. First, a thin layer of transparent conductive oxide (TCO) anode, specifically, indium-tin-oxide (ITO) was coated. Following layer of an uncharged conjugated polymer (PFPA-1) was used to improve device stability and to reduce the barrier at the organic/metal interface. Then a thin layer of active polymer-fullerene blend was spin-coated. In order to improve the charge transport and extraction from BHJ to the cathode, a layer of p-type organic semiconductor, such as PEDOT and PSS blend was used. The structure was completed with deposition of low work function metal, such as aluminum, which serves as the cathode. The finished device resulted in transparent structure, which is displayed in Figure 2.4.

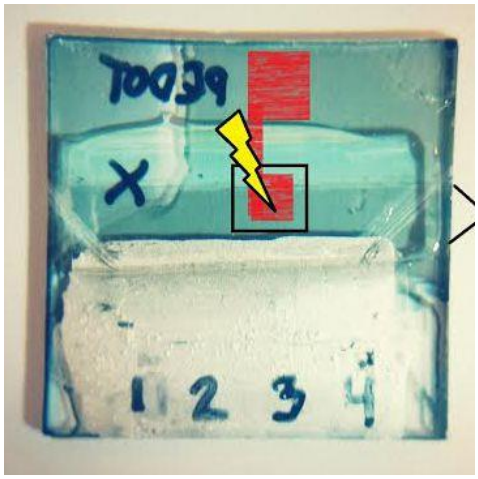

Figure 2.4. The solar cell device structure Glass/ITO/PFPA-1/polymer:fullerene/PEDOT:PSS(PH1000)/Glue/Glass. The yellow arrow marks the site of excitation, red area – ITO contact.

Since the structure of BHJ solar cell resembles an insulator between two metal electrodes, it can be described by the metal-insulator-metal (MIM) model, which is commonly used in explaining working regimes of the conventional solar cells. Due to low dielectric constant of the organic materials, the device with two metal electrodes acts like a capacitor with an induced electric field. The band diagrams provide the simplest explanation of organic solar cell working conditions under the applied electric field and light illumination. The effective conduction and valence band can be associated with the LUMO level of the acceptor (fullerene) and the HOMO level of the donor (polymer), respectively. This reveals one of the intrinsic properties of the organic semiconductors, where the effective band gap $E_{g,eff}$ of the blend differs from the optical band gap $E_{g,opt}$ of the polymer. The working functions (Φ) of the electrodes correspond to the conduction and valence bands, normally, high Φ_a for the anode and low Φ_c for the cathode. The energy band diagrams that correspond to the different working regimes are displayed in the Figure 2.5.

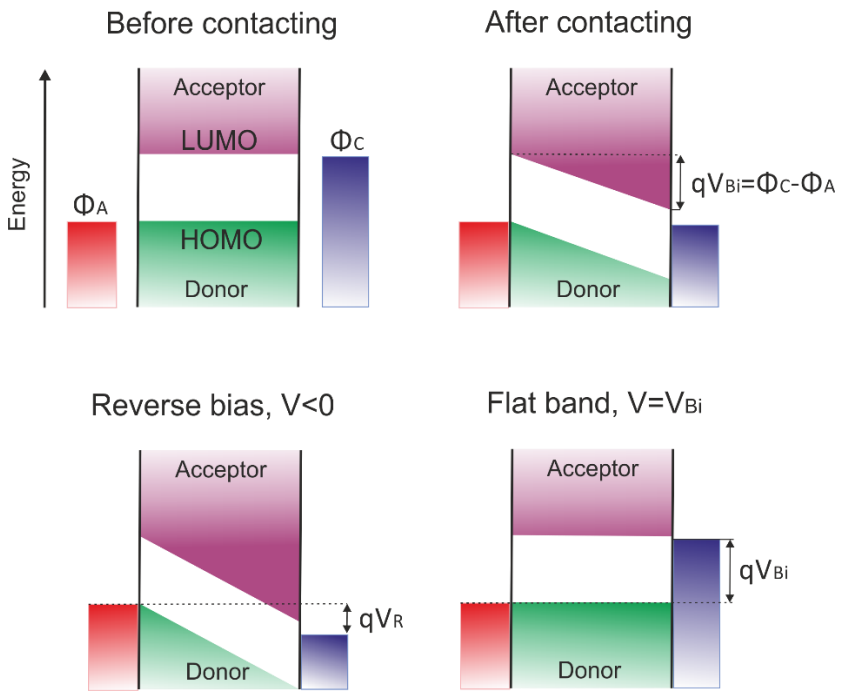

Figure 2.5. Energy band diagrams of the BHJ solar cell, where LUMO level of the acceptor correspond to the conduction band and HOMO level of the donor corresponds to the valence band. The anode with a low work function (Φ_a) and cathode with a high work function (Φ_c). The scheme represents four different working conditions: before contacting, after contacting (V=0), reverse and forward (flat band) biased cell. Application of contacts result in band shift (short circuit conditions) by the value of built in potential (V_{Bi}).

The application of contacts leads to higher energy electron diffusion from cathode to anode until the equilibrium is reached and the Fermi energy levels are in alignment throughout the whole system. As a result, the interfacial charges are formed near the electrode and organic layer junction (electrons near the anode and holes near the cathode). This alignment induces the local electric field ($qV_{Bi}= \Phi_c - \Phi_a$) in the photoactive layer, which is essential for charge dissociation and transport processes in the solar cells. The picture of the solar cell, when there is no external applied electric field ($V=0$) corresponds to short-circuit conditions. The application of reverse bias leads to an increase of total electric field ($q(V+V_{Bi})$) and hence increases the charge extraction from the photoactive layer, which is employed in organic photodetectors. In the situation, when the forward bias of the same magnitude as built in potential ($V= V_{Bi}$) is applied, the electric field in the active layer is canceled, resulting in the similar band diagram as of the separate BHJ layer and is refered to as flat band conditions. However, the built in potential does not describe the open circuit voltage (V_{OC}) of the organic solar cell in all the cases. Therefore, the effective band gap energy $E_{g,eff}$ = $LUMO_{Acceptor}$ - $HOMO_{Donor}$ in combination with charge recombination efficiency is usually used in order to define the open circuit voltage.

3 Photon-to-charge conversion in organic materials

In the previous chapters, the basic working principles of the bulk heterojunction solar cell were explained. The relatively low efficiency of organic solar cells is influenced by the variety of physical factors. Light absorption, which is usually an efficient process, is followed by formation of an exciton with high binding energy. In order to improve the efficiency of exciton dissociation an additional driving force is required, which, specifically in BHJ solar cells, is created due to offset between LUMO levels of donor and acceptor materials. The interface between two materials allows electron transfer and hence creation of a charge-transfer (CT) state with a significantly reduced barrier for charge generation. As the consequence, all initially generated excitons, which have diffused to the donor/acceptor junction, have higher possibility to dissociate into charges. However, the further processes of charge separation, transport and extraction are limited by the charge recombination that is reported to be relatively efficient in organic materials[4], [17]. Generally, the route from incidented photon to extracted charge is limited by collection of factors. A detailed description of the photo-generated processes will be presented in the following chapters.

3.1 Light induced processes

Absorption of light leads to excitation of the molecule with excess energy that will eventually relax backin to environment in a form emission of photons or thermal vibrations. A simplified scheme of the processes that proceed after light gets absorbed in a molecule is best illustrated by a Jablonski diagram, which can be seen in Figure 3.1.

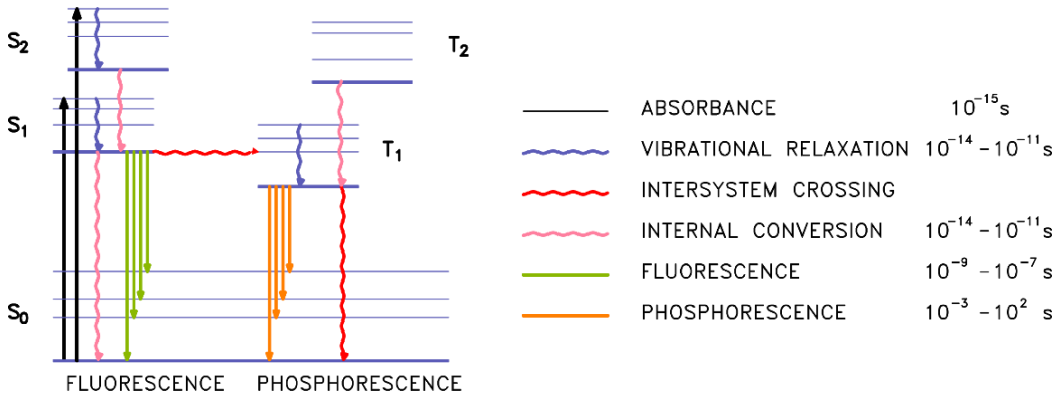

Figure 3.1. Jablonski diagram illustrating the most common photoinduced processes in molecules: absorption, vibrational relaxation (VR), internal conversion (IC), intersystem crossing (ISC), fluorescence (FL) and phosphorescence (Ph). Corresponding lifetimes of the processes are indicated. S_1, S_2 correspond to singlet, T_1, T_2 – triplet excited states.

Absorption of light leads to electronic excitation to S_n state as well as additional vibrational excitation depending on the energy of incident photon. Immediately, within hundreds of femtoseconds after excitation it follows the vibrational relaxation (VR) dissipating excess energy non-radiatively until

the lowest vibrational level of the excited state is reached. Good wave-function overlap between ground and excited states of the same multiplicity leads to internal conversion (IC), which may occur on the same timescale as VR. Intersystem crossing (ISC) occurs between states of different multiplicity (singlet (S_n) and triplet (T_n)) states is the slowest of all non-radiative transitions due to improbable magnetic interactions that involve electron spin flipping. However, strong spin-orbit coupling can result in high enough ISC rates to compete with IC [18], [19]. Other routes for energy to relax to the ground state are radiative transitions that occur through emission of photon. The photon energy corresponds to the energy difference of the emitting excited and the ground state. The transition between two singlet states ($Sn \rightarrow S_0$) is called fluorescence (FL) and typically occurs within nanoseconds. Phosphorescence occurs when the excitation relaxes from triplet to singlet ground state, which will again involves spin flipping, delaying the emission to µs – ms timescale. Overall, the processes that de-activate the excitation non-radiatively can be referred to as photoluminescence (PL) quenching and will be covered in detail in the later chapters.

3.1.1 Absorption and emission

Absorption of the specific wavelength occurs if the energy of a photon matches the difference between ground and one of the excited states. As a result, the electron of the lower energy occupied orbital is promoted to a higher unoccupied state orbital, which can often be referred as HOMO and LUMO orbitals, respectively. The absorption spectrum is determined by the overlap of the ground and the excited state wave-functions as it is shown in the Figure 3.2. The width of the spectrum correlates with conjugation length of the molecule. For instance, the broad absorption region in conjugated polymers is due to the variety of absorbing sites with different conjugation.

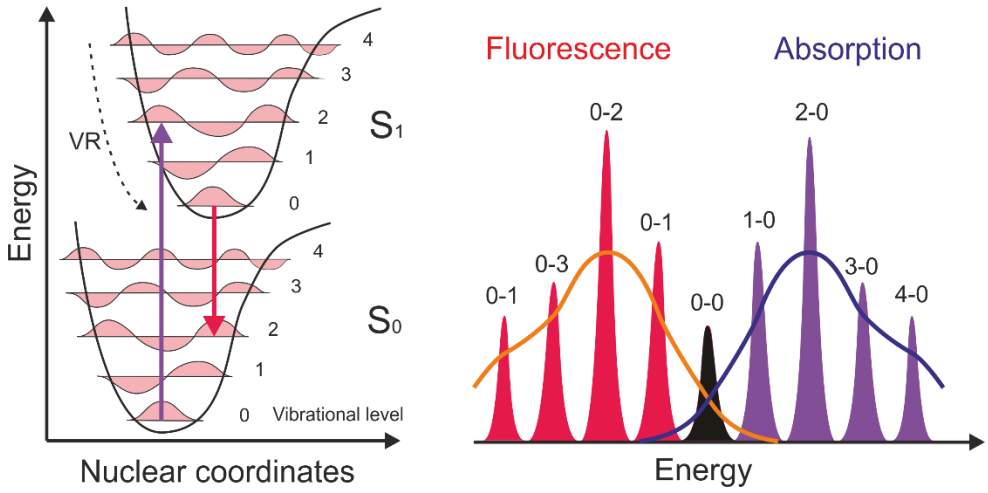

Figure 3.2. A Morse potential energy diagram showing the origin of the Stokes shift in terms of energy dissipation due to vibrational relaxation. The spectral distribution of the resulting absorption and emission is illustrated.

The transmitted intensity after absorption at the specific wavelength is given by the Beer-Lambert's law:

$$I(\lambda) = I_0(\lambda) \cdot 10^{-\epsilon(\lambda)cd} \quad (3.1)$$

where I_0 is the initial intensity, $\varepsilon(\lambda)$ is the molar extinction coefficient (in $M^{-1}cm^{-1}$), c is the molar concentration of the sample and d is the length light travels in the sample. Then the absorbance or the optical density (OD) value can be defined:

$$A = \varepsilon \cdot c \cdot d = -\log(\frac{I}{I_0}) \quad (3.2)$$

From the equation it follows that absorption has to scale linearly with intensity in order for the absorbance to be excitation intensity independent. For materials linear absorption coefficient is defined as $\alpha(\lambda)=\varepsilon(\lambda)c$. Typical absorption coefficient values for the organic materials are high (10^5 cm^{-1}), which allows thin (~100 nm) active layers in organic solar cells.

Absorption is followed by formation of an excited state, which can further relax in radiative and non-radiative pathways. Radiative emission of the photon (photoluminescence) could be subdivided into fluorescence and phosphorescence. Since photoluminescence is a relatively slow process and does not compete with vibrational relaxation, emission usually occurs from the lowest level of the excited state. This phenomenon is known as Kasha's rule. Another consideration that needs to be taken into account is the movement of the nuclei. Franck-Condon principle states that due to the relatively fast rate of optical transitions, the nucleus can be regarded as stationary, thus absorption and emission can be considered as vertical transition as shown in Figure 3.2. The photoluminance spectra is shifted to the lower energy side relative to absorption spectrum due to the extra energy which is dissipated via vibrational relaxation. Spectral shift is referred to as a Stokes shift. Normally the spectral structure is determined by the structure of the molecule. Monomers employing rigid structure usually exhibit highly pronounced vibrational peaks while relatively flexible polymers show relatively broad spectra without clear vibrational structure. The structure of the spectrum is also dependent on many other factors such as polarity of the environment, formation of bounded excited states in the neat films of the material or excitation energy transfer[18].

3.1.2 Excited state dynamics

Excited molecules, as all perturbed physical systems have to return to equilibrium within a characterized relaxation time. The dynamics of relaxation can be approximated by a first-order exponential law:

$$P_t = P_0 \times \exp(-kt) \quad (3.3)$$

According to this law initial population P_0 will decrease to population P_t within a time frame t with a reaction rate k.

The reaction rate k is expressed as a temperature T dependence of a reaction where reactants are transformed into products while acquiring a minimum amount of energy called the activation energy E_a. This information about the dynamics of the system can be extracted using Arrhenius equation:

$$k = A \cdot \exp(-E_a/RT) \quad (3.4)$$

here *R* is the ideal gas constant and *A* corresponds to frequency of the reaction. In the case of excited-state processes in a molecule *A* is associated with the vibrations and entropy of the atomic system. To provide information about the dynamics of the process, a reaction coordinate is used, where one or several coordinates of the nuclei represent the reaction path for the studied process. For one dimensional system a simplified scheme of reaction coordinate diagram can be drawn as shown Figure 3.3. The diagram features two states described by harmonic oscillators with a reorganization energy (λ), which can be defined as the energy required to reorganize the initial system and its environment in the event of the energy exchange.

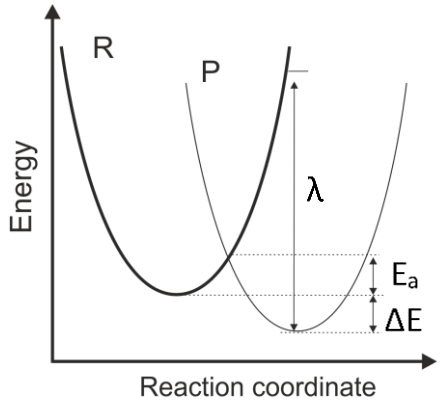

Figure 3.3. Schematic illustration of a one-dimensional reaction coordinate diagram between reactant and product states. The downhill energy transfer process has an activation energy E_a and a driving force ΔE.

The time it takes for the population to decrease to *1/e* of its initial value is defined by the decay lifetime τ, which is connected to reaction rate via $\tau=1/k$. The lifetime value can be experimentally observed by looking at decay kinetics that represent the decrease of photoluminescence intensity within a certain timescale after initial excitation. The decay processes usually consist of several components, which can be represented as a sum of reaction rates. Then it is useful to consider an experimentally observed lifetime:

$$\boldsymbol{\tau_{obs} = 1/\Sigma k_i} \quad (3.5)$$

where k_i represent all processes that deplete the initial population. For example, considering the decay of excited states in an organic molecule, the photoluminescence (PL) and excitation energy transfer (EET) would account for different decay rates. Therefore, when looking at decay kinetics of relatively slow photoluminescence any fast processes will lead to a decrease of the total lifetime and hence can be referred to as quenching processes. The efficiency of the processes can be represented by quantum yield that is determined as the ratio of the studied and total reaction rate.

3.1.3 Exciton generation and diffusion

At the time of photon absorption the electron is promoted from ground to excited state leaving an electron vacancy or the hole in the ground energy level. However, the electron and the hole remain strongly bound by Coulomb's force. This neutral bound excited state is referred to as exciton and can be viewed as a quasi-particle. According to Coulomb's law, the binding energy is

$$E_B = \frac{e^2}{4\pi\varepsilon_0\varepsilon_r r}, \quad (3.6)$$

where e is the elementary charge, ε_0 is the permittivity of the vacuum, ε_r – dielectric constant of the medium, and r is the distance between charges. As can be seen from the equation, the exciton binding energy is inversely proportional to the dielectric constant of the material. Since most of the organic materials are characterized with relatively low dielectric constants (ε_r ~2-4), the resulting exciton binding energy is high. Such excitons are referred to as Frenkel's excitons, with binding energies in the range of 0,1 - 0,5 eV. This is significantly higher than the thermal energy at room temperature (k_BT=0,025eV). As a consequence, little free charge carriers are formed due to exciton dissociation[20]. On the other hand, rising the temperature of the organic materials significantly increases charge generation efficiency.

To form free charge carriers in the BHJ solar cells, an exciton is required to reach the interface and dissociate within its lifetime (as illustrated in

Figure **2.2**). Thus, the exciton diffusion in the polymer medium is an essential process for efficient solar cell operation. The exciton energy transfer (EET) is defined as migration of the excited state between molecules without physically transferring the electron (Figure 3.4). Migration of the excitation is best described by Foster's energy transfer theory. There, it is assumed that energy is transferred through non-radiative dipole-dipole coupling. The energy transfer can be represented with a rate which depends on the overlap of the donor's fluorescence and acceptor's absorption spectra, the distance between donor and acceptor and relative orientation of the transition dipoles. Non-radiative energy transfer is one of the most important features of conjugated polymers where the lifetime of the process is in the timescale of hundred fs[21]. The actual electron transfer between donor and acceptor materials is another important process, on which the operation of polymer-fullerene solar cells rely. Electron transfer theory will be covered in the following chapters.

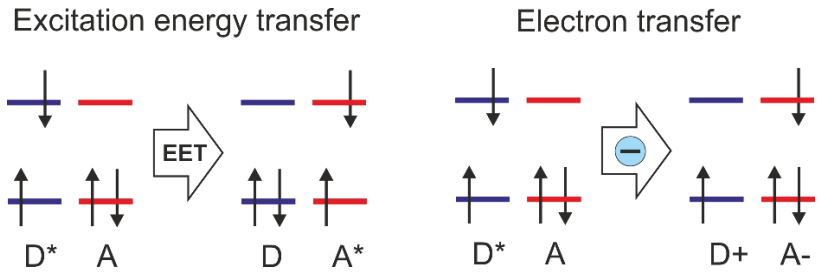

Figure 3.4. Illustration of excitation energy transfer (EET) and electron transfer processes. D* and A are excited donor and acceptor at the ground state. D+ and A- are donor and acceptor after electron transfer.

3.2 Charge photo-generation

Electron transfer is a different process from energy transfer since it involves physical migration of an electron from donor to acceptor molecule at BHJ interface (as shown in

Figure **2.2**). At this point, it could be said that the charges are already separated, however, evidence exist that the transferred electron is still bound to its hole that is positioned on the donor molecule. This bound state is usually referred to as charge transfer (CT) state which needs to dissociate in order to yield free charges.

3.2.1 Electron transfer theory

An electron transfer from donor to the acceptor is usually explained by the nonadiabatic electron transfer theory developed by Marcus[4]. Marcus' theory considers the reactant and product potential energy parabolas as two crossing harmonic oscillators, which were illustrated in Figure 3.3. The electron transfer should occur in the intersection of two parabolas, which correspond to the energy level and nuclear arrangement the reactant has to be in. Therefore, the electron transfer is an activated process with an activation barrier E_a, which is a function of the Gibbs free energy ΔE and the reorganizational coordinate λ:

$$E_a = \frac{(\lambda + \Delta E)^2}{4\lambda} \quad (3.7)$$

The rate for the electron transfer, k_{ET}, can thus be determined:

$$k_{ET} = \frac{2\pi}{h} \frac{|H|^2}{\sqrt{4\pi\lambda k_B T}} \exp\left(-\frac{(\lambda + \Delta E)^2}{4\lambda k_B T}\right) \quad (3.8)$$

Where H^2 is the electronic coupling between donor and acceptor states, h is Planck constant, k_B – Boltzman constant and T - the absolute temperature. From the formula it can be seen that due to exponential term, even little increase of the driving force for the process (ΔE) would influence a significantly higher electron transfer rate.

The product of the electron transfer in the donor/acceptor systems is the interfacial charge-transfer (CT) state, which is illustrated in **Error! Reference source not found.**. Here $\Delta E = E_{D^*} - E_{CT}$ is considered to be a driving force for exciton dissociation, where E_{CT} correspond to the LUMO level of the acceptor. The direct relation between CT state and parameters describing BHJ solar cell, such as, open circuit voltage (V_{OC}) and extracted photocurrent was reported[3], [4], [22]. The interest in CT state is caused due to its intrinsic characteristic of recombination directly to the ground state, meaning that the photoluminescence (even though of low energy and intensity) can be observed by sensitive measurement techniques[7], [22], [23]. Formation of the CT state was reported to be very fast (within 100 fs)[24], [25].

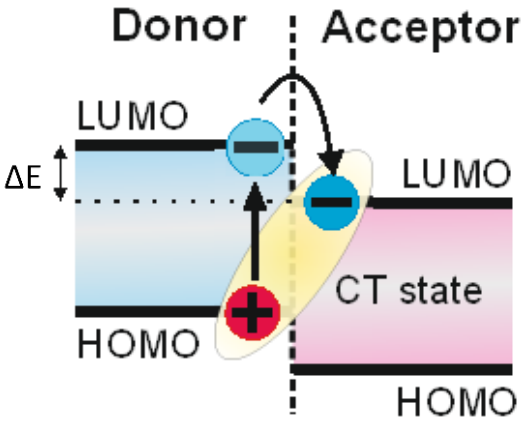

Figure 3.5. Energy level diagram of donor/acceptor interface illustrating the formation of a bound charge-transfer (CT) state. ΔE corresponds to the difference between LUMO energy levels (driving force for exciton dissociation).

3.2.2 Charge separation, transport and extraction

The further dissociation of coulombically bound CT state is well described by the Onsager-Braun's model. The theory is based on charge separation under an applied electric field, which allows for the electron-hole pair to overcome the Coulomb binding energy. The Onsager's model also describes the formation of "hot" states, when the higher excitation energy leads to the more efficient dissociation into charges. This is due to higher initial thermal energy that influences faster Brownian motion of the hot electron and hence the larger separation distance or thermalization length. Onsager also proposed that at the specific separation distance (Onsager's radius), where the Coulumb attraction energy equals thermal energy k_BT, the charge carriers are considered as fully separated. If the thermalization length is lower than Onsager's radius, the recombination of charges become more probable. Furthermore, the fully dissociated charges originating from different dissociated CT states can undergo the reversible process of recombination and formation of a new CT state. This is referred to as bimolecular recombination. Charge transportation towards electrodes in organic materials is illustrated as hopping between localized states (due to lack of long range order), instead of band transport found in crystalline semiconductors. As a consequence, the organic materials exhibit significantly lower charge mobility. However, the resulting low charge carrier mobility is not a major factor for organic solar cells, compared to other limiting effects. Charge transport, recombination and collection are beyond the scope of this thesis and are well described in the literature[3], [26].

The overall sequence from excitation of the polymer to extraction of charge can be represented as energy level diagram (Figure 3.6.). The photo-induced processes are marked as transitions between states with a certain reaction rate *k*, corresponding to the characteristic time of the process. The primary excitation of the S_n state in the polymer is created by light absorption and is referred to as an exciton. The exciton then has several pathways to give off his energy. If exciton is excited with high energy, there is a possibility for direct charge separation (CS, direct) from "hot" exciton states. However, usually due to fast processes of internal conversion (IC) and vibrational relaxation (VR)

most transitions occur from thermally relaxed states. From relaxed S_1 state exciton can either recombine radiatively (PL) or begin charge generation by transferring electron to the acceptor molecule. Prior to electron transfer, the exciton has to diffuse within a polymer phase with a rate of excitation energy transfer (EET) until it reaches the donor-acceptor interface. The formation of "hot" charge-transfer (CT) state is possible, depending on the lowest excited energy level (LUMO) difference of the donor and acceptor. Bound electron-hole pairs in the "hot" CT state can separate into free charges directly or relax vibrationaly to the lowest CT level, from where most of the charge separation (CS) processes take place. The main limiting factors, leading to energy losses are the geminate recombination (GR) of bound electron-hole pair and bimolecular recombination (BR) of the free charges. The free charges that did not recombine are transported through percolation pathways to the electrode, where they are extracted.

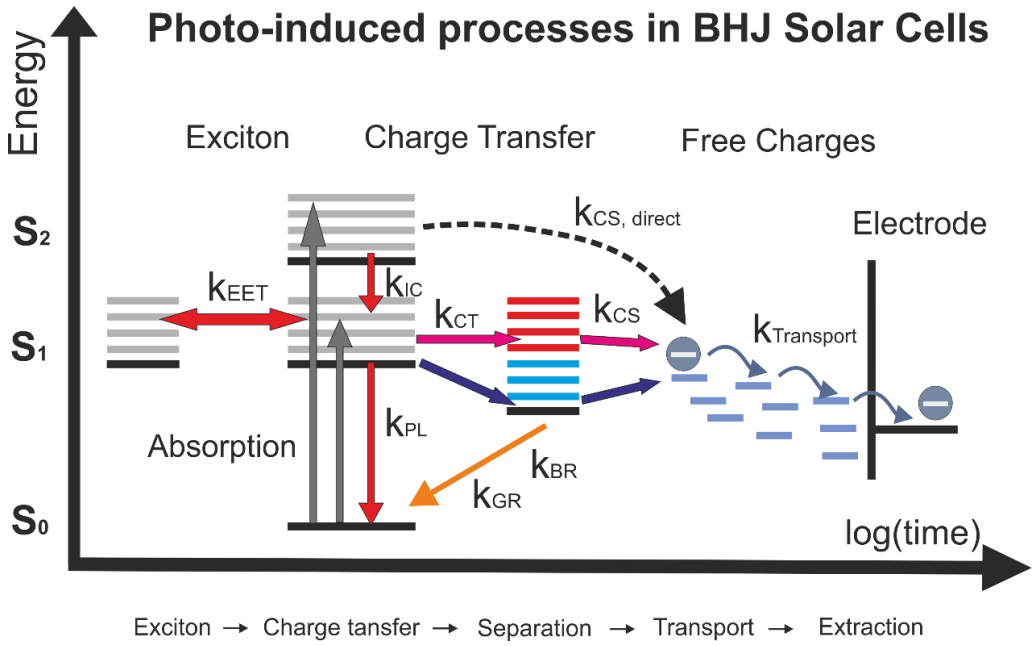

Figure 3.6. Photo-induced processes of BHJ solar cells in an energetic perspective.

4 Techniques and methodology

4.1 Sample preparation

In this Thesis work, low band-gap polymers, in particular **PTI-1** (E_g=1,6 eV) and **P3TI** (E_g=1,5 eV) were studied. Blending polymers with fullerene resulted in BHJ solar cells with different driving forces. The PTI-1 polymer was mixed with both $PC_{61}BM$ and $PC_{71}BM$ in the ratio 2:3 and 1:2, respectively, in order to optimize the morphology of the blends. The PTI-1:$PC_{71}BM$ is considered as a more efficient active layer due to its higher absorption in the visible range and higher driving force for exciton dissociation[15]. P3TI:$PC_{71}BM$ 2:3 blend was chosen since recent studies reported a relatively high driving force of 0.1 eV as well as solar cell power conversion efficiencies up to 6%[22], [27].

The samples were fabricated and characterized by our collaborators in Prof. Olle Inganäs' group in the Centrer of Organic Electronics, Linkoping University, Sweden. Samples included neat films of the PTI-1 and P3TI polymers placed in between glass substrate, the films of three polymer-fullerene blends (PTI-1:PC61BM, PTI-1:PC71BM, P3TI:PC71BM) and the solar cells of the same blends. The solar cell device structure is a sequence of layers: Glass/ITO/PFPA-1/polymer:fullerene /PEDOT:PSS(PH1000)/Glue/Glass.

4.2 Time-resolved photoluminescence measurements

A streak camera setup is used to measure time-resolved photoluminescence of the samples on the scale of picoseconds. One of the prominent features of the setup is the ability to measure spectral and temporal distribution at the same time. This is an outcome of intricate sequence of the processes, modifying the initial beam of photoluminescence. The setup consists of four main parts: laser pump system, spectrograph, streak camera and CCD camera.

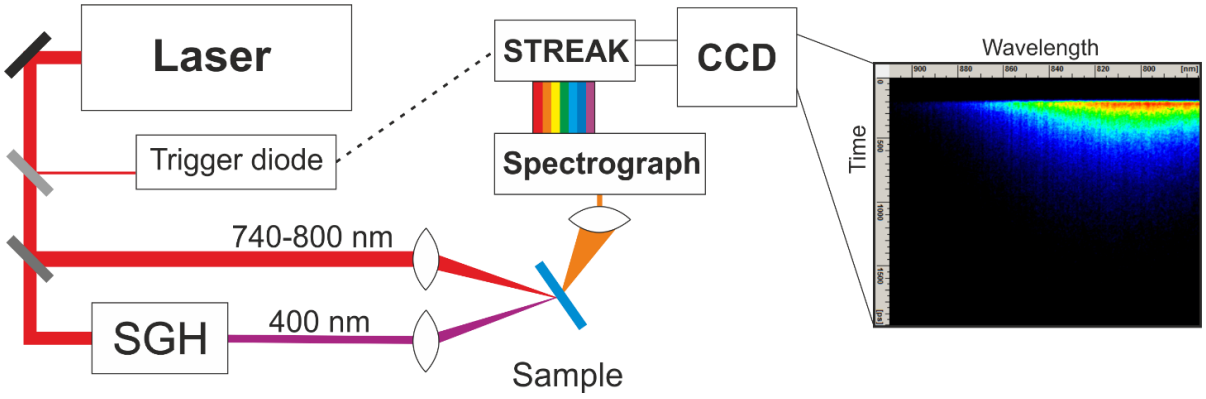

Figure 4.1. Schematic illustration of the STREAK camera setup. The resulting two dimensional picture is presented on the right.

First, the sample is excited with short impulses that were produced by laser system. The setup consisted of a 532 nm laser (Millennia Pro) pumping a passively mode-locked Ti:Sapphire oscillator (Tsunami), providing ~100 fs pulses at 80 MHz repetition rate with a wavelength of 800 nm. A small portion of the output is directed to the trigger photodiode while the rest goes to lithium triborate (LBO) crystal. The second harmonic generation process results in double the initial excitation energy (400 nm). If the sample excitation requires excitation in the red region (740 nm), the unit of second harmonic generator (SGH) is skipped. The beam after generation is taken through various neutral density filters and optical lenses to reduce the intensity and focus the excitation beam on the sample.

The resulting photoluminescence of the sample is collected through a series of lenses and focused onto a vertical slit before entering the spectrograph (Cromex), where grating system provides spectral distribution in the horizontal plane. The beam with horizontal spectral information is then sent through the horizontal slit to the streak camera (Hamamatsu). There, photons hit the photo-cathode and produce the special distribution of electrons corresponding to initial wavelength of the photon. Electrons are then accelerated towards the streak tube, where a very fast sinusoidal time-dependent voltage is applied in the vertical plane. The trigger mechanism is used to synchronize the sinusoidal function of the voltage with the repetition rate of the laser. As the changes of the voltage are very quick, the time-correlated incoming photoelectrons are deflected differently by electric field, resulting in time-dependent vertical distribution. Then the combination of microchanel plate and phosphor screen is used to amplify the signal and convert electrons back to photons. The final stage is photon detection with a CCD camera (Hamamatsu). The result is a two-dimensional image with spectral distribution on the horizontal axis and temporal distribution on the vertical axis. The temporal resolution can be changed by horizontal slit before streak camera and amplitude of the voltage.

5 Formation and diffusion of an exciton in a polymer material

Absorption of light in the polymer material leads to creation of a neutral bound excited state or Frenkel exciton. The excited state is formed by binding few monomer units in the same molecule and creating a chomophore as it is shown in Figure 5.1 (a). Polymers have the property to form different conjugation segments or chromophores with different binding energy that can be excited with corresponding excitation wavelength.

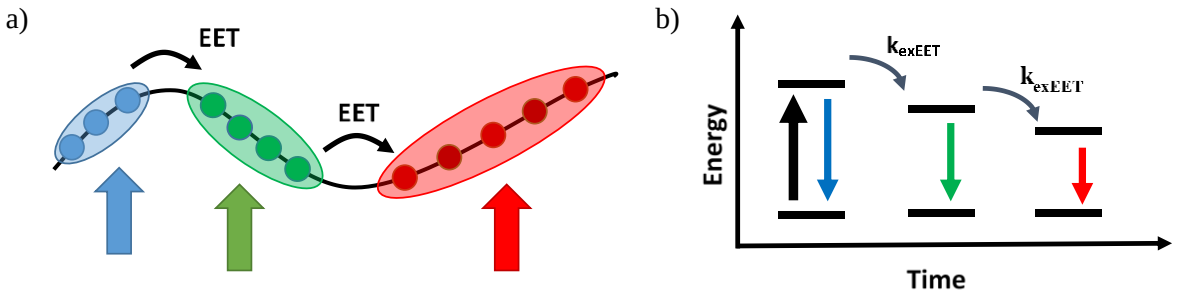

Figure 5.1. a) Illustration of three intramolecular chromophores in a polymer chain. Colored arrows indicate excitation at different energy. Black arrows indicate excitation energy transfer (EET). b) Shematic band diagram of the charge transfer processes.

The heterogeneous distribution of chromophores with different energies leads to broadening of the absorption and emission spectra and thus allows fast excitation energy transfer (EET) from high energy chromophores to other sites corresponding to low energy. The theory of excitation energy transfer is well described by Forster's theory (see Chapter 3.1.3). Downhill energy transfer in a single polymer chain (intrachain) is a very rapid process, normally with the characteristic time of few ps[28]. Energy transfer can also occur between nearby chains (interchain energy transfer). The latter is usually observed in the polymer films with tightly packed polymer molecules or coiled single polymer chains. Therefore, the fast energy transfer processes allow for the exciton to migrate in the polymer phase within its lifetime and reach the polymer-fullerene interface. This is one of the main requirements for efficient charge generation in polymer-fullerene solar cells.

5.1 Excitation energy transfer

Experimentally, energy transfer can be observed by ultrafast time resolved photoluminescence (TRPL) studies. The decay dynamics of the higher energy emission of the excited states should contain a faster decay component due to a fast downhill energy transfer between conjugated elements. Correspondently, at the red side of the emission spectrum one can observe a rise of the emission intensity. Figure 5.2 represents the kinetic decay of PTI-1 and P3TI polymer materials. In both cases, the fast decay component (τ~10 ps) is easily distinguished in the higher energy (780-800 nm) photoluminescence regions, which corresponds to emission from higher energy chromophores. Therefore, the initial photoluminescence is quenched by fast non-radiative process of energy transfer. Probing at the red side of the emission spectra (880-900 nm) results in approximately single exponential photoluminescence decay (Red lines in Figure 5.2) with a lifetime of 150ps for PTI-1 and 100 ps for P3TI. This decay can be assigned to radiative recombination of the lowest lying excited state. The faster photoluminescence decay rate for P3TI suggests a presence of more efficient quenching process, for instance, efficient exciton dissociation or internal conversion and intersystem crossing.

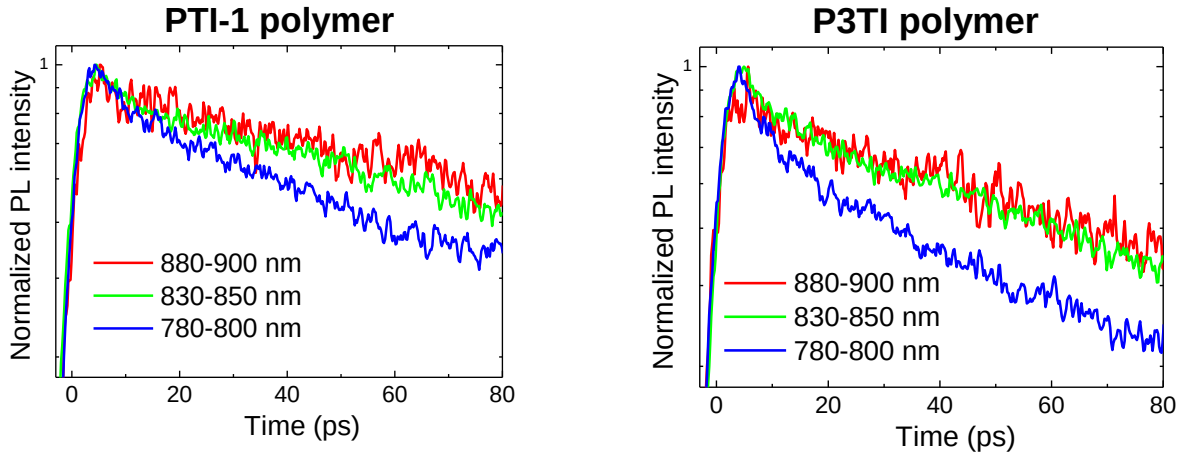

Figure 5.2 The integrated kinetic traces for different wavelength regions of PTI-1 and P3TI polymers at short time scale. Samples were excited at 740 nm wavelength.

To provide a better insight into energy transfer processes, the same neat polymer films were excited with higher energy λ=400nm (3,1eV) light. According to the earlier picture (Figure 5.1), this should lead to excitation of higher energy chromophores and result in more pronounced energy transfer. More blue-shifted emission spectra compared to the one obtained with the lower excitation energy would be a clear evidence of a heterogeneous distribution of the chromophores. Higher contribution of the fast component while measuring PL decay at shorter wavelength (Figure 5.3) indicates the increase of energy transfer that is observed upon 400 nm excitation.

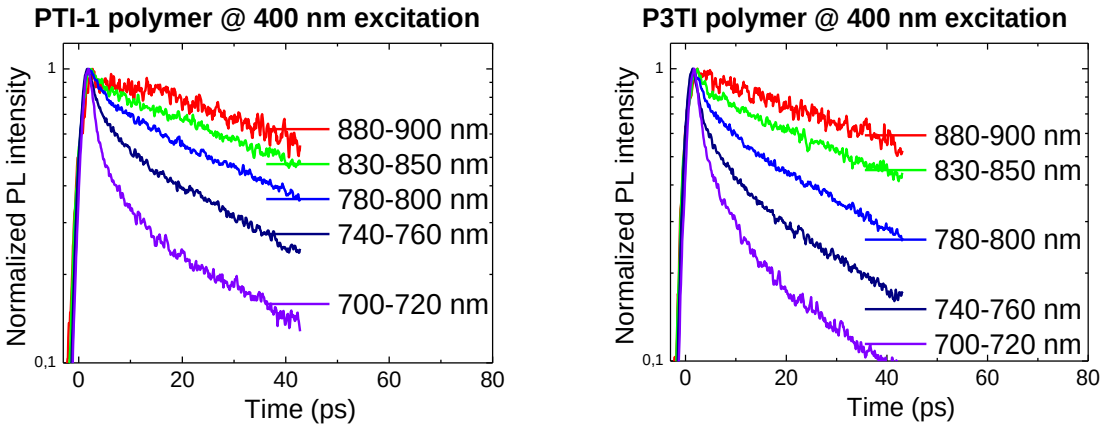

Figure 5.3. The integrated kinetic traces for different PL emission regions of PTI-1 and P3TI polymers at short time scale. Samples were excited at 400 nm wavelength.

Energy transfer processes can be more easily visualized as shifts of emission spectra peaks to the lower energy region. Figure 5.4 represents normalized photoluminescence of both polymers at three different time ranges, each with a certain delay after initial excitation. The red-shift of the PL peak at 100-300 ps delay represents higher emission intensity from lower energy excited regions (chromophores) in the polymers. This result is a clear indication of energy transfer, earlier illustrated in Figure 5.1 (b).

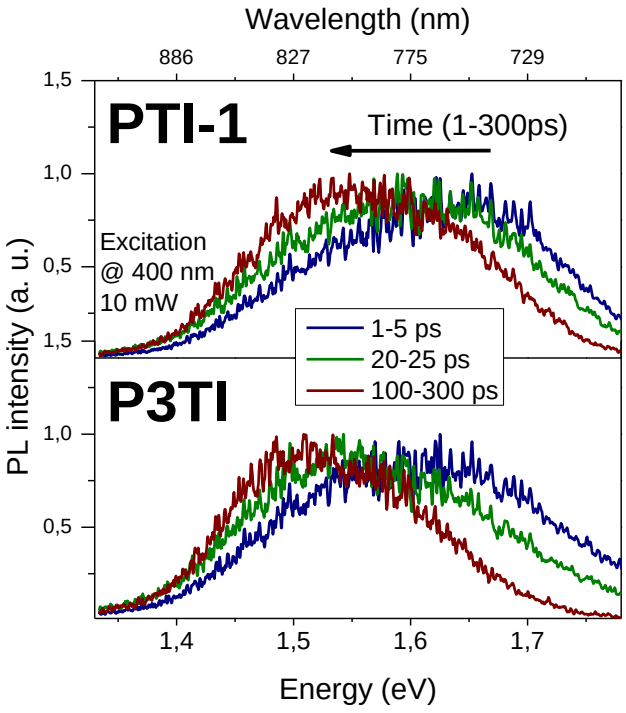

Figure 5.4. Emission spectra of the polymers measured with a delay after the initial excitation. Samples were excited at 400 nm wavelength.

The contribution of the fast decay as well as the red-shift of the PL is more pronounced for P3TI polymer compared to PTI-1, which provides an idea about higher rate of the energy transfer in the neat P3TI polymer films. To confirm the observations of the energy transfer processes in polymer material an additional time resolved anisotropy experiments were performed.

5.2 Emission anisotropy decay

The time dependent photoluminescence polarization anisotropy measurements is a powerful tool to detect the effects of molecular rotation, Brownian motion or energy transfer between molecules with different orientation. In the case, when rotational and translational motions of chromophores are frozen in a rigid polymer films, the depolarization effect observed is solely caused by a non-radiative energy transfer between chromophores. Since the transition dipole moments of the chromophores in polymer are in general not parallel, the polarization of the emitted photoluminescence is affected by the energy transfer. This can be observed as a depolarization of the emitted light compared to the excitation light. The information on the time dependent excitation transport is related to the decay of the emission anisotropy, which is defined as:

$$r(t) = \frac{I_{\parallel}(t) - I_{\perp}(t)}{I_{\parallel}(t) + 2I_{\perp}(t)} = \frac{I_{\parallel}(t) - I_{\perp}(t)}{I(t)} \qquad (5.1)$$

where $I_{//}$ and $I_{\perp}$ are the polarized components parallel and perpendicular to the direction of polarization of the incident light, and I is the total fluorescence intensity. In the case of motionless molecules with random orientations, when the emissive state is excited the emission anisotropy is r_0=0,4 and is called the fundamental anisotropy[18]. The decay of the emission anisotropy of an indirectly (via Forster's energy transfer) excited chromophore varies with time, usually approaching zero value[29]. This leads to the assumption that excited population of the polymer films should initially exhibit a decay of the stationary molecular system. Therefore, the time dependent anisotropy should start with a value of 0,4 at time zero and decay to zero at later times. However, measurements of the time dependent anisotropy decay for PTI-1 and P3TI polymers (Figure 5.5) revealed that the initial value of anisotropy is 0,1 and 0,17, respectively.

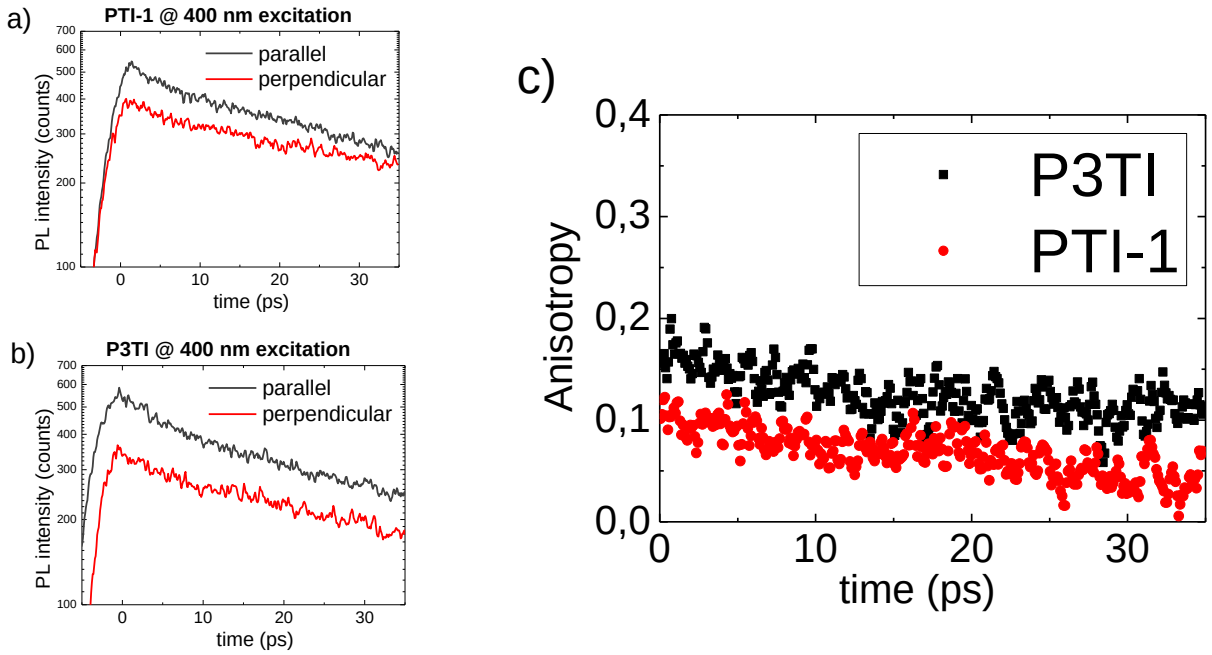

Figure 5.5. Kinetic decay spectra of the polymers PTI-1 (a) and P3TI (b) when the emitted light is measured at parallel and perpendicular polarization relative to excitation polarization. (c) represents the anisotropy decay of the same polymers calculated from the emission intensities.

One of the possible explanations is that due to the instrumental function, which reduces the time resolution of the measurements, the faster decay component induced by the energy transfer cannot be resolved and thus the initially observed photoluminescence is already partially depolarized. Since the decay of the polarization anisotropy is visible in 1-40 ps time region, the assumption of even faster component would lead to energy transfer model with two possible pathways. As literature suggests, the faster component could be assigned to intra-chain energy transfer between chromophores of the same polymer molecule, while energy transfer on the longer timescale is due to inter-chain transitions between different molecules.

On the other hand, orientation of the dipoles of different excited states is the intrinsic property of the molecule, dependent on its electronic structure. The dipole moments of the transitions between first excited state and ground state (absorption and emission) are always to be parallel. The excitation at higher energies may also excite higher lying energy states, which have transition dipole moments that are not necessarily parallel to the absorption dipole moment of the first excited state. Thus the fast internal conversion process between the states with different dipole orientations would result in decreased the initial value of the anisotropy. The analysis of the absorption spectra of the polymers (Figure 5.6) suggests that excitation at 400 nm may involve othe electronic transitions from the higher lying electronic states. To reduce the influence of the higher lying states it is preferential to excited polymers at the energy corresponding to the approximate band gap energy.

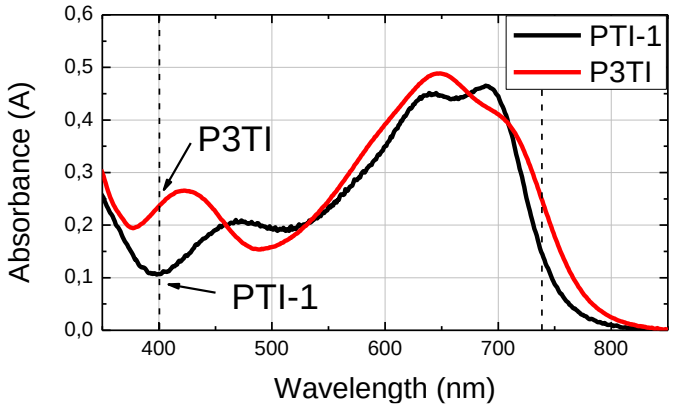

Figure 5.6. Steady-state absorption spectra of PTI-1 and P3TI polymers. Arrows indicate absorption at 400 nm.

Overall, detailed investigation of the two similar polymer systems resulted in a clear indication of differing excitation energy transfer properties. The polymer-fullerene blends incorporating P3TI polymer should exhibit more efficient charge generation due to faster exciton diffusion and hence a higher chance for an exciton to reach the dissociation sites at the interface of polymer and fullerene. However, inhomogeneity of the polymer phase and morphological properties, which normally differ for blends, also strongly influence the way exciton would diffuse to the interface.

6 Exciton dissociation in polymer-fullerene blends

Large exciton binding energy in neat polymers leads to high exciton dissociation barrier which can be lowered by increasing the driving force. The required driving force can be increased by applying an electric field, which naturally induces an electric force on charges and increases a chance of exciton dissociation. The other option is to introduce a good electron accepting material (for example, fullerene). Mixing a polymer with fullerene molecules was found to significantly increase the exciton dissociation yield. The extra driving force is provided by the lower LUMO level of an acceptor in relation to the LUMO level of the donor (polymer), which is illustrated in the Figure 3.5. Polymer exciton that has migrated to the polymer-fullerene interface will undergo a very fast (τ_{CT} ~ 100 fs) dissociation by electron transfer to the acceptor material[3], [30]. This will result in a coulombically bound donor and acceptor molecules or so called charge transfer (CT) state.

The formation of free charges then can be viewed as further dissociation of the CT state. Since after the CT dissociation charges are no longer bound by the Coulombic force they are free to migrate to the electrodes of the solar cell where they can be extracted. However, charge recombination remains a possible pathway for formation of a new bound CT state which can further recombine radiatively or non-radiatively. The processes of recombination of charges cannot be observed by the photoluminescence measurements and therefore require a highly sensitive transient absorption measurements. The effects of charge recombination are well described in the following literature [3], [4], [21].

6.1 Observations of the Charge generation in Polymer-fullerene blends

Time resolved photoluminescence (TRPL) measurements only provide the information on the emitting states, in our case, the radiative decay of the lowest lying excited state in the polymer. Emission from other excited states, such as CT or higher excited states are difficult to detect due to their relatively short lifetime and low radiative emission quantum yield. Therefore, observations of time dependent photoluminescence allow to refer to quenching processes that deplete the initial excited population in the non-radiative pathways by reducing the amount of states that recombinate radiatively.

The information about exciton dissociation and charge generation processes can be obtained from photoluminescence measurements. Normally, photoluminescence in polymer materials corresponds to a radiative recombination of the exciton that did not dissociate into charges during its lifetime. Introduction of an additional driving force results in higher possibility for the same polymer excitons to split into charges. This processes that reduces the photoluminescence can be referred to as quenching of polymer excitons. Therefore, the comparison of photoluminescence in neat polymer and in polymer-fullerene blends provides information about charge generation process.

The effect of photoluminescence quenching is demonstrated in Figure 6.1. The influence of charge generation on a reduction of lifetime of PL is easily observable for P3TI:PC71BM blend when

comparing it with pure P3TI polymer, Figure 6.1 (a). In the previous chapter (see page 19) it was proved, that polymer emission at 880-910 nm region does not show the influence of fast energy component. Therefore, the only process that could influence the faster decay in polymer:fullerene blends is exciton dissociation. Interestingly, the PTI-1 polymer-based blends indicated a negligible change of photoluminescence dynamics, which disagrees with the reports of noticeable photoluminescence quenching in the same polymer-fullerene systems[22].

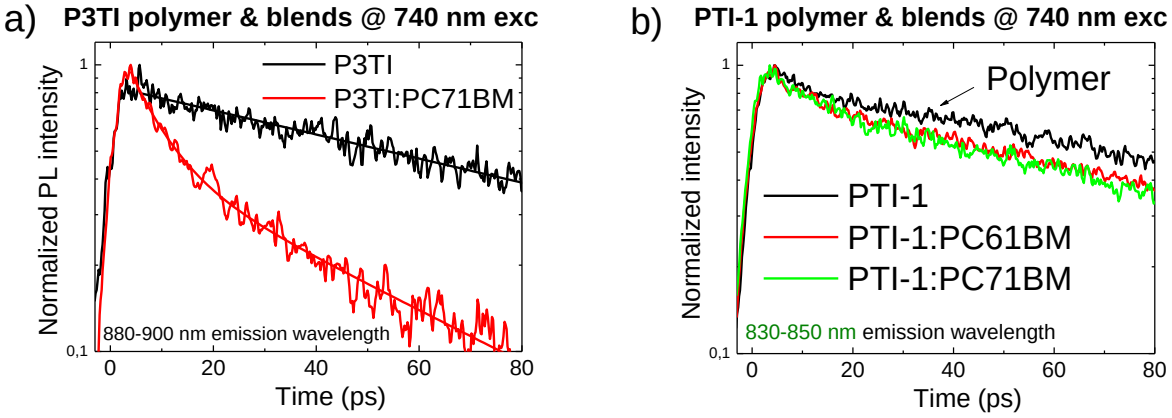

Figure 6.1. Comparison of kinetic decays for (a) P3TI (b) PTI-1 polymers and their fullerene blends. Samples were excited with 740 nm wavelength light.

The observations of low PL quenching in the PTI-1 polymer-based blends leads to an assumption that exciton dissociation is an inefficient process due to high energy barrier. However, this picture would disagree with the fact that solar cells produced with PTI-1:PCBM blends as an active layer exhibited noticeable charge generation under illumination. Thus, the possible concept of equilibrium between forward and backward electron transfer needs to be considered. Since the driving force for the PTI-1:PCBM blends was measured to be around 0 eV, the efficient electron back transfer from CT state to polymer exciton is probable. The influence of interfacial driving force is easily observable for P3TI:PC71BM blend, where the energy difference between LUMO of the polymer and LUMO of the fullerene was measured to be 0,1 eV. Significant quenching of the photoluminescence suggests an efficient charge generation process at the polymer-fullerene interface.

It was proved that the presence of the electron acceptor can significantly increase the efficiency of excitons dissociation, depending on the magnitude of the driving force at the interface of the materials. In the following chapters, the efficiency of charge generation in polymer-fullerene solar cells will be investigated as the function of excess thermal energy (“hot” states) or applied electric field.

6.2 Hot exciton states

The absorption of higher energy photons in conjugated polymers results in formation of higher energy excitons which can undergo a fast downhill energy transfer process to the lower energy sites as it was proven in energy transfer section. However, some reports suggest that prior to vibrational relaxation to the lowest excited state or energy transfer to the other chromophores, the charge generation from thermally "hot" excitons can occur[31]–[33]. This suggests that creation of bound charge-transfer (CT) state is overcome in polymer-fullerene blends, leading to direct separation free electron and hole pairs, as it was illustrated in Figure 3.6. The excess thermal energy allows for the electron-hole pair to overcome the Coulombic attraction force in terms of a Boltzman process[32]. Dissociation of "hot" excitons into free charges must be a very fast process since it is in direct competition with energy transfer and vibrational relaxation of excess energy. The relaxation to the lowest lying excited state is normally followed by the formation of an interfacial CT state, which will be discussed in the following section.

Indication of "hot" exciton states can be verified experimentally by exciting pure polymers and blends with excess energy relative to their first excited states and later comparing the charge generation yield with one that was calculated for low energy excitation. The quantum yield for quenching by charge generation can be expressed with a simple formula:

$$QY_{CG} = \frac{QY_{Polymer} - QY_{Blend}}{QY_{Polymer}} \quad (6.1)$$

where QY represents the photoluminescence quantum yield of polymers and their fullerene blends. The quantum yield of the specified process can also be derived from the photoluminescence decay rates:

$$QY_{CG} = \frac{k_{Polymer} - k_{Blend}}{k_{Polymer}} \quad (6.2)$$

Here the decay rates k correspond to the lifetime of the photoluminescence decay in simple relation $k=1/\tau_{1/e}$. Since radiative recombination of the excited states is a single exponential process, the approximate lifetime ($\tau_{1/e}$) can be extracted from the decay dynamics of the photoluminescence at the 1/e intensity of the decay kinetics as it is displayed in Figure 6.2.

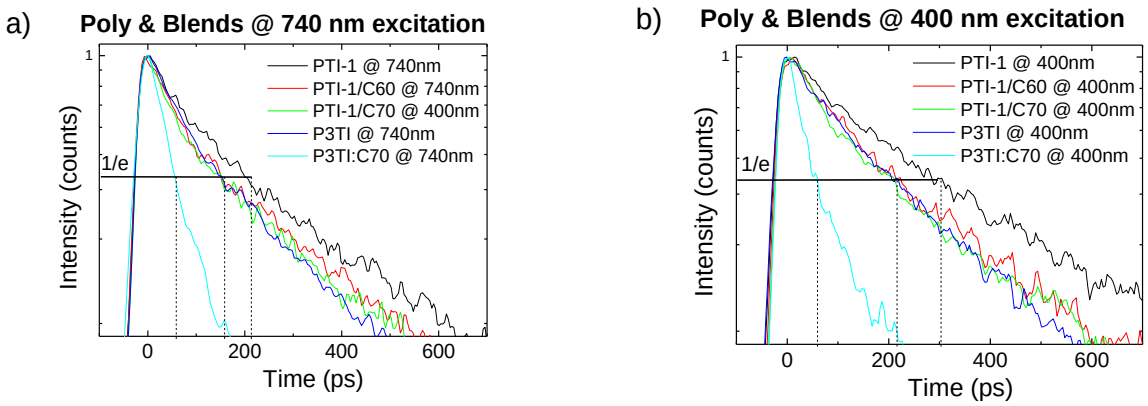

Figure 6.2. The photoluminescence decay kinetics of PTI-1 and P3TI and their fullerene blends for 740 nm (a) and 400 nm (b) excitation wavelength.

Initially, polymer:fullerene blend samples were excited with 740 nm (1.7 eV) light which corresponds to the lowest excited state transition in the polymer materials. Thus, the effects of the direct high energy exciton dissociation into charges could be ignored. The excitation with 400 nm (3.1 eV) creates thermally "hot" exciton states, which could result in more efficient direct dissociation into free charges. The calculations for the charge generation quantum yield in polymer:fullerene blends are shown in Table 6.1.

Table 6.1. Calculation of charge generation quantum yields Q_{CG} in PTI-1 and P3TI blends.

	400 nm				740 nm				
	$\tau_{1/e}$	$k_{1/e}$	k_{CG}	Q_{CG}	$\tau_{1/e}$	$k_{1/e}$	k_{CG}	Q_{CG}	$\frac{Q_{CG}\ (400\ nm)}{Q_{CG}\ (740\ nm)}$
PTI	304	0,003			215	0,005			
P3TI	216	0,005			152	0,007			
PTI/C60	226	0,004	0,001	**0,257**	160	0,006	0,002	**0,256**	**1,00**
PTI/C70	207	0,005	0,002	**0,319**	155	0,006	0,002	**0,279**	**1,14**
P3TI/C70	60	0,017	0,012	**0,722**	56	0,018	0,011	**0,632**	**1,14**

The final quantitative measure of dissociation from "hot" exciton states is derived as a ratio of the quantum charge generation yields for different excitation energies. The calculations provided similar QY_{CG} values for all blends indicating little effect of excess excitation energy and the absence of direct "hot" exciton dissociation into free charges. This finding suggests that the process of vibrational relaxation to the first excited state is significantly faster and therefore results in efficient thermalization of charges, being in agreement with recent reports[34]. Due to energy relaxation to the first excited state of the polymer, the only plausible pathway for exciton to dissociate is an electron transfer to a fullerene molecule. This process leads to formation of an electron-hole pair at the polymer-fullerene interface also called charge-transfer (CT) state, as it was shown in **Error! Reference source not found.**. Further, the influence of the difference between LUMO levels of the polymer and CT state will be discussed. This separation between levels was proven to be the main driving force for charge separation. Inducing an electric field in the material is followed by shifting of the LUMO levels, thus further decreasing the barrier for charge formation.

6.3 “Hot” charge-transfer states

In the case of the formation of “hot” CT states a similar logical pathway as for dissociation from “hot” excitons could be applied, which was discussed in the previous section. However, this time the generation of free charges occurs not from polymer excitons but by dissociation of charge-transfer (CT) states, as illustrated in Figure 6.3. Analogically, the excited CT state has a manifold of vibrational levels. Therefore, the charge transfer (k_{CT}) into higher energy levels leads to a temporal formation of thermally “hot” excited CT state. Further dissipation of the excess energy can occur via fast vibrational relaxation process (k_{VR}) to the lowest excited CT state which is normally followed by charge generation process ($k_{CG,\ cold}$). The generated charges can be transported to the respective electrode by hopping between localized states ($k_{Transport}$) or can recombine back into CT state and later to the ground state (k_{CR}). However, recent studies report the possible pathway for “hot” CT state to dissociate into charges more efficiently[33], [35]. The direct separation of electron-hole pair ($k_{CG,\ hot}$) can overcome the potential barrier of the Coloumbic attraction force.

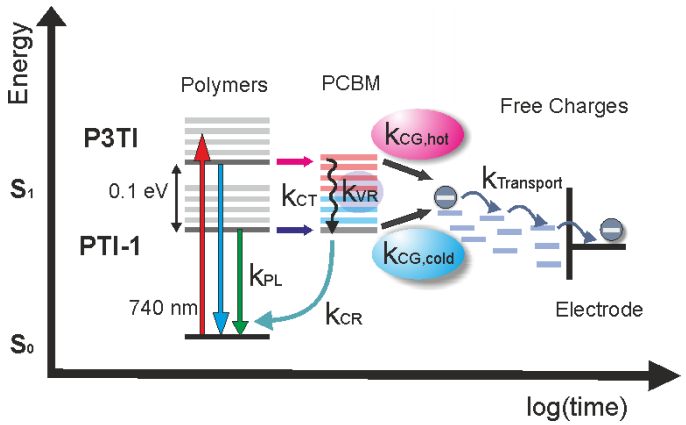

Figure 6.3. Schematic illustration of charge generation processes in PTI-1:PCBM and P3TI:PCBM blends.

The generation of CT states normally occurs via charge transfer from a polymer exciton to an acceptor (PCBM) molecule at the polymer-fullerene interface. The “hot” CT states can be formed when there is an energy difference between lowest lying excited states or LUMOs of both materials, which is also called “driving force”. In our case, the relative difference of the driving forces for PTI-1:PC61BM and P3TI:C71BM polymer-fullerene blends was measured to be around 0.1 eV. Therefore, the transition to the CT manifold from the P3TI polymer has better chances to result in “hot” CT formation.

Similarly to the calculations in the previous section, the comparison of a polymer and its blend provides information about interfacial charge generation in the polymer-fullerene blends. The excitation near the band gap of the polymers (740 nm) was applied to reduce the influence of energy transfer in polymers as well as to eliminate the possibility of a direct charge generation from “hot” exciton states. Since all generated charges will result from dissociation of CT states, the previous charge generation quantum yield (Q_{CG}) (see Chapter 6.2) will now be referred to as the efficiency of

exciton dissociation (η_{ExD}). To be able to compare the processes of CT dissociation into charges the additional parameter describing the performance of the polymer-fullerene hetero-junction in the solar cells is needed.

Earlier measurements performed by Prof. Inganäs from Linkoping University, provided information on the overall efficiency of the solar cells. Devices were produced by incorporating the same PTI-1:PC61 and P3TI:PC71BM blends as an active layer of a cell. The obtained external quantum efficiency (EQE) can be represented as the product of the efficiency of the photo-physical processes in a solar cell[3]:

$$EQE = \eta_{abs} \cdot \eta_{ExD} \cdot \eta_{CTSD} \cdot \eta_{FCT} \cdot \eta_{CE} \quad (6.3)$$

where η_{abs} represents the efficiency of photon absorption and exciton generation, η_{ExD} – exciton dissociation, η_{CTSD} – charge transfer state dissociation, η_{FCT} – free charge transport, and η_{CE} – charge extraction. The product of the last four parameters provides the internal quantum efficiency (IQE) or the absorbed photon-to-current conversion efficiency. The IQE of the solar is calculated by accounting for differences of exciton generation in the polymer medium because it is the main absorbing material in the BHJ solar cell. Since the exciton generation for the PTI-1 and P3TI polymers differs at particular absorption wavelength, the absorption coefficients were obtained from steady-state absorption spectra (see Figure 5.6). Absorbance value provides an approximate ratio of the excitons created for the photons absorbed also called the quantum yield of exciton generation (η_{abs}). Assumption has to be made that all absorbed photons result in excitation of the conjugated polymer.

In order to directly compare CT dissociation (η_{CTSD}) processes in both material systems notion on the generated charge transport (η_{FCT}) and extraction (η_{CE}) must be made. Since all investigated solar cells were produced utilizing same material layers for charge transport and collection (see page 6), η_{FCT} and η_{CE} values are considered as constant and will not affect further calculations. Processes of the charge carrier hopping and extraction in organic materials are beyond the scope of this discussion and are well described in the literature[3], [4], [36].

Finally, the calculated IQE values are assumed to reflect the number of dissociated CT states from the total amount of excitons that were generated. Dividing IQE by the exciton dissociation efficiency (η_{ExD}) should result in approximate values for CT state dissociation (η_{CTSD}). The calculations are displayed in the Table 6.2.

Table 6.2. Calculations of charge-transfer (CT) dissociation efficiency (η_{CTSD}) for polymer-fullerene blends.

	$\tau_{1/e\ (ps)}$	$\kappa_{1/e}$	κ_{CT}	η_{ExD}	EQE (%)	η_{abs}	IQE (%)	η_{CTSD}
PTI	215	0,005						
P3TI	152	0,007						
PTI-1:PC61BM	160	0,006	0,0016	0,256	0,626	0,15	4,17	**0,163**
P3TI:PC71BM	56	0,018	0,0113	0,632	2,825	0,25	11,30	**0,179**

The obtained charge-transfer dissociation efficiency values were comparable for PTI-1:PC61BM (η_{CTSD} = 16,3 %) and P3TI:PC71BM (η_{CTSD} = 17,9 %) were comparable considering the instrumental function of the measurement techniques. Similarities in CT dissociation suggest the absence of the "hot" CT states of the free charge generation channel. Otherwise, significantly higher η_{CTSD} value for

P3TI:PC71BM system holding 0,1 eV higher driving force would have been observed. The results also reveal that process of relaxation in the manifold of the CT vibrational levels (k_{VR}) is notably faster than direct dissociation of CT into free charge carriers. Further investigation on the effects of driving force will include the electric field dependence measurements of the polymer-fullerene BHJ systems.

6.4 Role of electric fields in driving charge generation

An exciton that is primarily generated in a polymer is described as Frenkel exciton and features a relatively high binding energy. Therefore, pure polymer material normally exhibit efficient exciton dissociation only when sufficiently strong electric fields are applied[7], [22]. Introduction of electron accepting fullerene leads to a formation of charge transfer (CT) state, where the electron and hole are separated by some distance due to charge localization on different molecules. As a result, the binding energy decreases and even low applied electric fields are sufficient to break the bound state and separate charges. The studies of the electric field dependence of the CT state reveals the limiting factors of the charge generation process such as a dissociation barrier and charge recombination.

Application of an electric field induces an additional driving force (ΔE) for exciton dissociation into CT states. It can be visualized as a relative movement of the potential energy surfaces of the donor exciton (D*/A) and CT state (D_+/A_-) (Figure 6.4). Higher driving force influences the reduction of the barrier for electron transfer. The initial barrier height is defined by the reorganizational energy that is described by Marcus theory (see section **Error! Reference source not found.**). The reorganization energy can be defined as the energy required to reorganize the initial system and its environment when the electron transfer occurs.

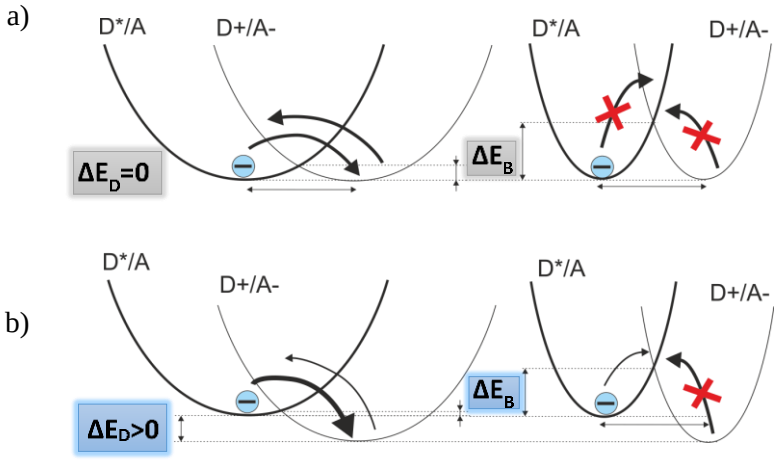

Figure 6.4. Potential energy surfaces describing possible electron transitions from polymer exciton (D*/A) to CT state (D_+/A_-). The influence of driving force (ΔE) caused by electric field is shown as (a) when no electric field is present, $\Delta E=0$ and (b) electric field is applied, $\Delta E>0$. Models represented illustrate the cases of low (left) and high (right) reorganizational energy.

The case of low reorganizational energy results in low barrier for exciton dissociation, however, the electron back-transfer to the polymer exciton is as efficient as transfer to CT state. The introduction of an electric field disturbs the equilibrium and the filling of CT becomes more efficient. The model with high reorganizational energy employs a high barrier which prohibits electron transfer both ways. This implies that only sufficiently high electric fields permit population of CT state, which will further dissociate into charges.

Direct observations of CT state photoluminescence (PL) in polymer-fullerene systems have been previously reported[23], [37]. However, sensitive measurement techniques are required due to low PL recombination quantum yield of the CT state. The alternative route is to observe a pathway of Frenkel exciton radiative recombination of a polymer exciton. The application of an electric field creates a PL quenching effect, which indirectly indicates the more efficient exciton dissociation into CT states.

In our case, the dynamics of photoluminescence as a function of electric field was investigated. The initial excitation wavelength of 740 nm was applied, which corresponds to the lowest lying excited state of the polymer. Due to the low PL emission of the solar cells, the integration of the whole emission spectrum was necessary in order to obtain satisfactory signal-to-noise ratio. The PL decay measurements displayed in Figure 6.5 (a) reveal the kinetics that can be fitted as a double exponential decay. The fast component (τ_1~12 ps) exhibited no change with electric field (Figure 6.5 (b)) thus it can be assigned to the fast energy transfer in the polymer material (see Chapter 5.1). On the contrary, the longer component showed a clear electric field dependence. The increase of the reverse bias resulted in shorter decay times, indicating quenching of the polymer exciton.

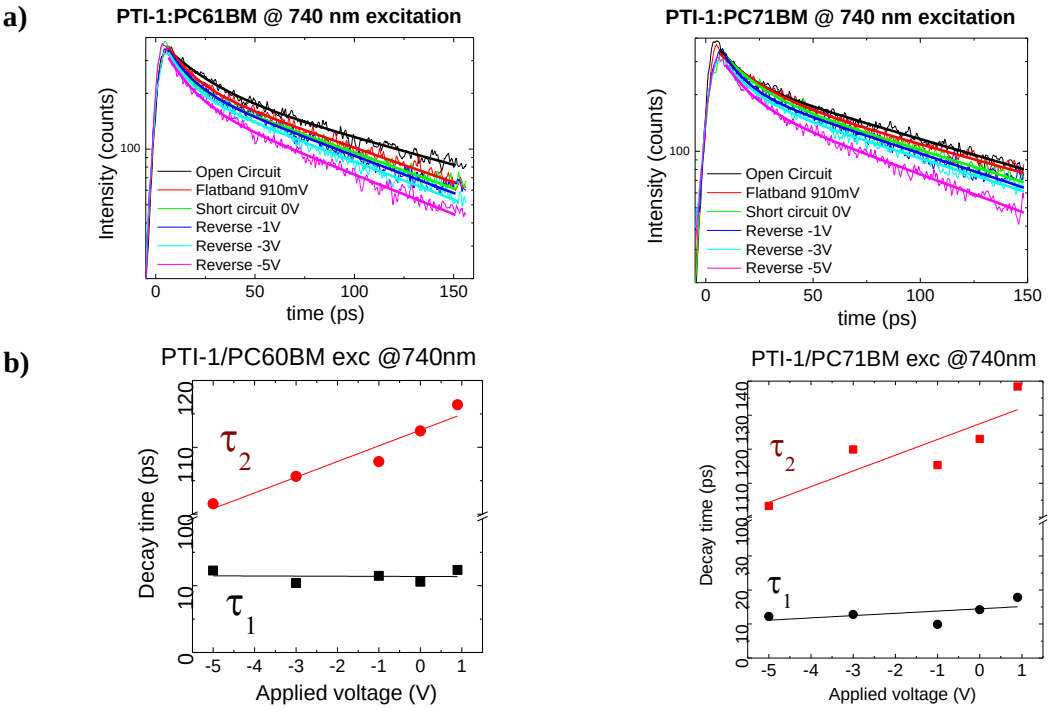

Figure 6.5. (a) Kinetic decays of PTI-1:PC61BM and PTI-1:PC71BM solar cells measured at applied electric field. (b) Fitted decay times (τ_1 and τ_2) and their dependence on the applied electric field.

In order to directly compare different polymer-fullerene systems the quenching ratio was obtained by integrating the detected counts of biased cell photoluminescence spectra ($PL_{applied\ bias}$) and relate it to the integrated PL spectra of the flat band conditions (explained in Figure 2.5) $PL_{flat\ band}$:

$$PL\ Quenching\ ratio = \frac{PL_{Applied\ Bias}}{PL_{Flat\ Band}} \quad (6.4)$$

The results are displayed in Figure 6.6. When excited at 740 nm both material systems exhibited linear dependence to electric field, which is in agreement with photocurrent measurements (Figure 6.7). This correlation allows to assume that dissociation of the polymer exciton is directly related to generation of the charges.

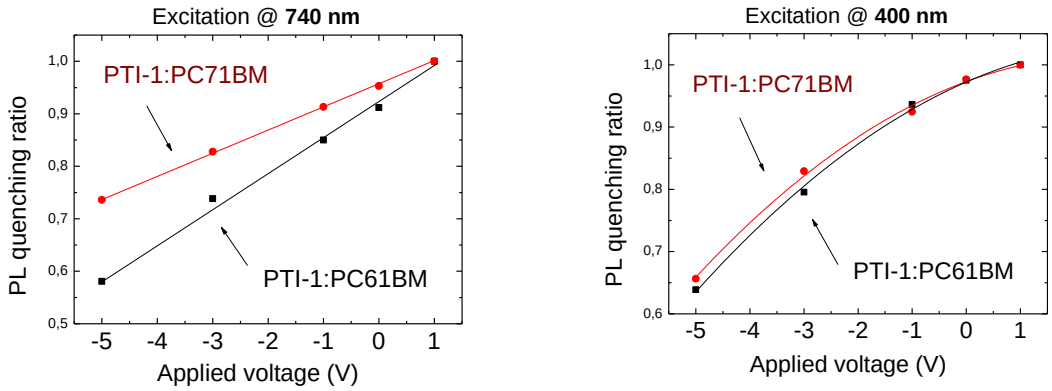

Figure 6.6. Photoluminescence quenching measurements for PTI-1:PC61BM and PTI-1:PC71BM solar cells. The samples were excited with 740 nm (left) and 400 nm (right) excitation wavelength.

The less pronounced quenching effects due to applied electric field in PTI-1:PC71BM solar cell suggest the slightly higher natural driving force which causes slightly higher exciton dissociation efficiency as compared to PTI-1:PC61BM blend. This is confirmed by better solar cell performance (Table 1). On the contrary, the excitation of the same solar cells with higher energy photons (400 nm) resulted in similar quenching dynamics.

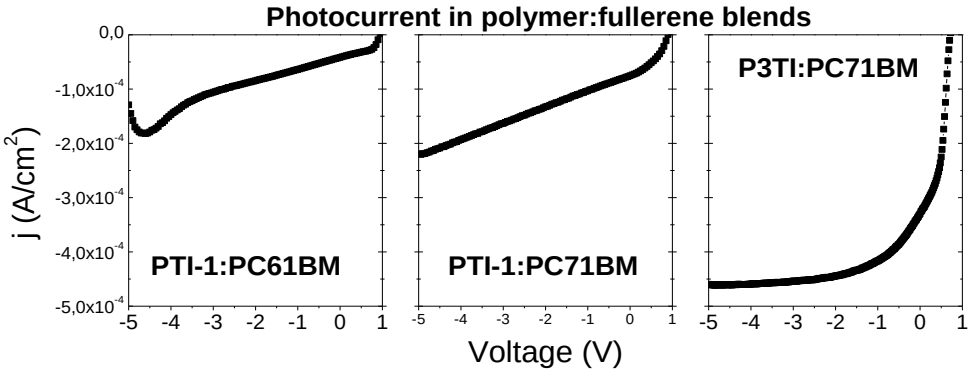

Figure 6.7. Photocurrent measurements for three polymer: fullerene blend based solar cells. Measurements were performed by Prof. Inganäs from Linkoping University.

Time resolved photoluminescence measurements of P3TI:PC71BM solar cell exhibited no applied electric field dependence at the given voltage region (Figure 6.8), which is in agreement with high photocurrent at low electric fields (Figure 6.7) as well as earlier photoluminescence quenching studies[22]. The photoluminescence decay displayed a fast component of 8 ps, which as discussed earlier is due to an efficient exciton dissociation at the polymer-fullerene interface (see Chapter 6.1). Application of an electric field induces an additional force driving exciton dissociation, however, the lack of response to electric field indicates that the majority of the polymer excitons dissociate already at 0.1 eV driving force at the interface of the polymer-fullerene blend. Controversially, this suggests the exciton binding energy of P3TI polymer is lower than 0.1 eV, which is significantly less than indicated in other studies of the conjugated polymer systems[38], [39].

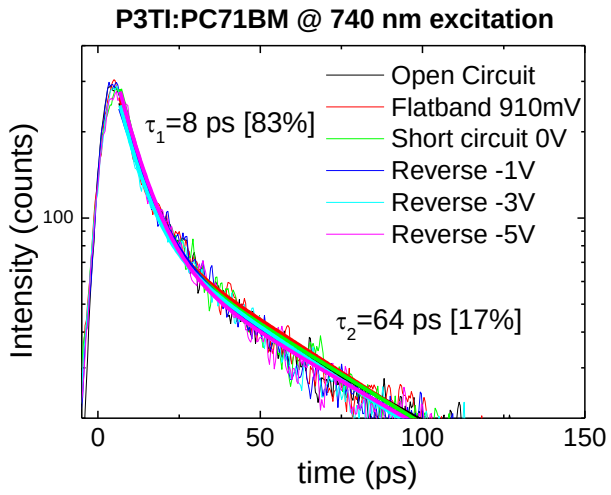

Figure 6.8. Decay kinetics of the P3TI :PC71BM solar cell at different applied electric fields.

The electron transfer processes in P3TI:PC71BM blend can be well described by the earlier picture of potential energy surfaces with low reorganizational energy (see Figure 6.4). In this case, the product potential well is low enough for activational barrier to be negligible and for the electron back transfer to be a fairly inefficient process. On the contrary, the interfacial driving force of 0 eV for the PTI-1 polymer-based blends leads to assumption that even though the barrier is low, the efficient back transfer is present. Thus, the recombination of the dissociated excitons is more efficient than separation of charges, which is in agreement with the observations of fast (τ_{CT}~100fs) formation and dissociation of charge-transfer state[30]. The applied electric field disturbs the balance by increasing the barrier for back transfer and increasing a chance of further dissociation into free charges.

Summary

The work in this thesis was focused on physical charge photo-generation processes in organic bulk heterojunction (BHJ) polymer-based solar cells. Investigation of time resolved photoluminescence (TRPL) allowed to identify rapid processes that are essential steps in charge separation mechanism. Initially, the study of neat films of two isoindigo-based polymers revealed a fast (~10 ps) energy transfer process which is on the similar timescale as previously reported values. The additional measurements of anisotropy decay in pure polymers showed the clear evidence of exciton diffusion, however, the unresolvable initial value indicated the possible faster energy transfer component. That would be in agreement with two step (intrachain and interchain) energy transfer model. Clear evidence of downhill energy transfer confirmed a model of heterogeneous chromophore distribution in polymer phase. Direct comparison of PTI-1 and P3TI polymers revealed a more pronounced energy transfer component for P3TI, which agrees with its longer conjugation length due to planar molecular structure.

Further studies included the investigation of polymer and fullerene blends, which due to introduction of electron acceptor had a reduced barrier for exciton dissociation into charges. Photoluminescence quenching studies revealed a clear charge generation in P3TI-based blend, which was measured to have 0.1 eV driving force for excitons dissociation into CT states. The PTI-1 polymer-based blends exhibited a negligible exciton dissociation due to equilibrium between donor and acceptor energy levels. Therefore, the model with low reorganizational energy was suggested, which stated that efficient back electron transfer to the polymer exciton is possible because of low activation barrier. Electric field studies of the same BHJ solar cells, confirmed previous assumption since the increase in charge generation was observed under small applied electric field. No electric field dependence for P3TI-fullerene blend lead to conclusion that majority of excitons are dissociated by 0.1 eV driving force and thus the binding force of the excitons is of the same magnitude.

The possible pathways of direct charge generation from higher energy states were studied by exciting polymers and their blends with higher energy photons. Results suggested that relaxation processes (VR an IC) are on the much faster timescale (<100 fs) than exciton dissociation to charge-transfer state or further CT state dissociation into free charges. Therefore, no “hot” state charge generation was observed in P3TI and PTI-1 polymer based BHJ systems.

Self-reflection

In the course of the project I had to achieve goals in certain areas, such as, understanding of the matter (Physics); planning, critical thinking and problem solving; understanding and explaining the relevance of the project in the society. The project began by studying the relevant literature based on the basic concepts behind the photogeneration processes as well as recent researches. The difficulty I encounterd here was the current state of the photo-generation theory in organic materials, which is complex and thus not fully determined for most of the material systems. Therefore, some of the outcomes of the experiments were difficult to predict.

Second step included the learning of methodology and techniques as well as how to apply them for the specific problem. The crash courses in the ultrafast time-resolved absorption and photoluminescence spectroscopy provided the knowledge of the experimental methods that extended beyond my field of study, however, it will be necessary in the further studies. Since the whole study had to be carried out in the limited amount of time with limited resources, the thorough plan had to be prepared prior to performing the experiments. The lack of personal expertise in carrying out complex experiments resulted in questionable outcome and therefore some of the experiments had to be repeated.

After having acquired all the data, the analysis and characterization of the observed phenomena began. One of the main mistakes was the separation of the analysis and experimental part, which lead to collection of excess data that was not used for explaining the physical phenomena. Since the project was a part of collaboration with researchers from Linkoping University, the skills of communication in scientific language and collaborative work were improved. Nonetheless, the major part of the research was carried out autonomously, with guidelines provided by the supervisor.

Overall, the opportunity to perform a research in a relevant field of studies provided a broader outlook of the problem. This lead to understanding of current limitations and possibilities for the future research. Few of the main lessons I personally learned, when working in one of the leading groups in the field of organic electronics, included the fine work ethics in the scientific environment as well as the effective approach to the scientific problem.

Acknowledgements

I would like to thank my supervisor Arkady for providing support and guiding me through complex world of organic material science. I also want to thank my second supervisor Wei Zhang, who helped with technical part of the project as well as exchanged ideas in the further steps of the project. Many thanks to our collaborator Armantas Melianas from Linköping University who provided the samples for the research and supported my findings. I would also like to thank all the people in Chemical Physics department for the possibility to always be able to disscuss scientific issues.

References

[1] *Global Market Outlook for Photovoltaics 2012-2017*. European Photovoltaic Industry Association, 2013.

[2] K. Branker, M. J. M. Pathak, and J. M. Pearce, "A review of solar photovoltaic levelized cost of electricity," *Renew. Sustain. Energy Rev.*, vol. 15, no. 9, pp. 4470–4482, Dec. 2011.

[3] C. Deibel and V. Dyakonov, "Polymer–fullerene bulk heterojunction solar cells," *Rep. Prog. Phys.*, vol. 73, no. 9, pp. 1–39, Sep. 2010.

[4] T. M. Clarke and J. R. Durrant, "Charge Photogeneration in Organic Solar Cells," *Chem. Rev.*, vol. 110, pp. 6736–6767, 2010.

[5] P. Boland, K. Lee, and G. Namkoong, "Device optimization in PCPDTBT:PCBM plastic solar cells," *Sol. Energy Mater. Sol. Cells*, vol. 94, no. 5, pp. 915–920, May 2010.

[6] H. van Eersel, R. a. J. Janssen, and M. Kemerink, "Mechanism for Efficient Photoinduced Charge Separation at Disordered Organic Heterointerfaces," *Adv. Funct. Mater.*, vol. 22, no. 13, pp. 2700–2708, Jul. 2012.

[7] K. Tvingstedt, K. Vandewal, F. Zhang, and O. Inganäs, "On the Dissociation Efficiency of Charge Transfer Excitons and Frenkel Excitons in Organic Solar Cells : A Luminescence Quenching Study," *J. Phys. Chem. C*, vol. 114, pp. 21824–21832, 2010.

[8] K. Vandewal, K. Tvingstedt, A. Gadisa, O. Inganäs, and J. V Manca, "On the origin of the open-circuit voltage of polymer-fullerene solar cells.," *Nat. Mater.*, vol. 8, no. 11, pp. 904–9, Nov. 2009.

[9] B. D. Wohrle and D. Meissner, "Organic Solar Cells," *Adv. Mat.*, vol. 3, pp. 129–138, 1991.

[10] T. N. Foundation, "The Discovery of Polyacetylene Film : The Dawning of an Era of Conducting Polymers," *Angew. Chem. Int. Ed.*, no. 40, pp. 2574–2580, 2001.

[11] J. a. Bartelt, Z. M. Beiley, E. T. Hoke, W. R. Mateker, J. D. Douglas, B. a. Collins, J. R. Tumbleston, K. R. Graham, A. Amassian, H. Ade, J. M. J. Fréchet, M. F. Toney, and M. D. McGehee, "The Importance of Fullerene Percolation in the Mixed Regions of Polymer-Fullerene Bulk Heterojunction Solar Cells," *Adv. Energy Mater.*, vol. 3, no. 3, pp. 364–374, Mar. 2013.

[12] F. C. Jamieson, T. Agostinelli, H. Azimi, J. Nelson, and J. R. Durrant, "Field-Independent Charge Photogeneration in PCPDTBT/PC 70 BM Solar Cells," *J. Phys. Chem. Lett.*, vol. 1, no. 23, pp. 3306–3310, Dec. 2010.

[13] F. C. Krebs, S. a. Gevorgyan, and J. Alstrup, "A roll-to-roll process to flexible polymer solar cells: model studies, manufacture and operational stability studies," *J. Mater. Chem.*, vol. 19, no. 30, p. 5442, 2009.

[14] H. Chen, J. Hou, S. Zhang, Y. Liang, G. Yang, and Y. Yang, "Polymer solar cells with enhanced open-circuit voltage and efficiency," vol. 3, no. November, pp. 649–653, 2009.

[15] E. Wang, Z. Ma, Z. Zhang, P. Henriksson, O. Inganäs, F. Zhang, and M. R. Andersson, "An isoindigo-based low band gap polymer for efficient polymer solar cells with high photo-voltage.," *Chem. Commun. (Camb).*, vol. 47, no. 17, pp. 4908–10, May 2011.

[16] E. Wang, L. Hou, Z. Wang, S. Hellström, W. Mammo, F. Zhang, O. Inganäs, and M. R. Andersson, "Small band gap polymers synthesized via a modified nitration of 4,7-dibromo-2,1,3-benzothiadiazole.," *Org. Lett.*, vol. 12, no. 20, pp. 4470–3, Oct. 2010.

[17] S. D. Dimitrov and J. R. Durrant, "Materials Design Considerations for Charge Generation in Organic Solar Cells," 2014.

[18] B. Valeur, *Molecular Fluorescence. Principles and Applications*, vol. 8. 2001.

[19] K. Sato, K. Shizu, K. Yoshimura, A. Kawada, H. Miyazaki, and C. Adachi, "Organic Luminescent Molecule with Energetically Equivalent Singlet and Triplet Excited States for Organic Light-Emitting Diodes," *Phys. Rev. Lett.*, vol. 110, no. 24, p. 247401, Jun. 2013.

[20] Y. Infahsaeng, *Light induced charge generation, recombination, and transport in organic solar cells / Yingyot Infahsaeng*. Lund : Department of Chemical Physics, Lund University, 2013, 2013.

[21] T. Österman, *Excited State Processes in Solar Energy Materials*. Lund : Department of Chemical Physics, Lund University, 2013, 2013.

[22] K. Vandewal, Z. Ma, J. Bergqvist, Z. Tang, E. Wang, P. Henriksson, K. Tvingstedt, M. R. Andersson, F. Zhang, and O. Inganäs, "Quantification of Quantum Efficiency and Energy Losses in Low Bandgap Polymer:Fullerene Solar Cells with High Open-Circuit Voltage," *Adv. Funct. Mater.*, vol. 22, no. 16, pp. 3480–3490, Aug. 2012.

[23] M. Hallermann, S. Haneder, and E. Da Como, "Charge-transfer states in conjugated polymer/fullerene blends: Below-gap weakly bound excitons for polymer photovoltaics," *Appl. Phys. Lett.*, vol. 93, no. 5, p. 053307, 2008.

[24] C. J. Brabec, G. Zerza, G. Cerullo, S. De Silvestri, S. Luzzati, J. C. Hummelen, and S. Sariciftci, "Tracing photoinduced electron transfer process in conjugated polymer / fullerene bulk heterojunctions in real time," vol. 340, no. June, pp. 232–236, 2001.

[25] S. De, T. Kesti, M. Maiti, F. Zhang, O. Inganäs, A. Yartsev, T. Pascher, and V. Sundström, "Exciton dynamics in alternating polyfluorene/fullerene blends," *Chem. Phys.*, vol. 350, no. 1–3, pp. 14–22, Jun. 2008.

[26] A. Pivrikas and R. O. , N. S. Sariciftci, G. Juska, "A Review of Charge Transport and Recombination in Polymer / Fullerene," *Prog. Photovolt.*, vol. 15, no. 15, pp. 677–696, 2007.

[27] E. Wang, Z. Ma, Z. Zhang, K. Vandewal, P. Henriksson, O. Inganäs, F. Zhang, and M. R. Andersson, "An easily accessible isoindigo-based polymer for high-performance polymer solar cells.," *J. Am. Chem. Soc.*, vol. 133, no. 36, pp. 14244–7, Sep. 2011.

[28] J. G. Müller, J. M. Lupton, J. Feldmann, U. Lemmer, and U. Scherf, "Ultrafast intramolecular energy transfer in single conjugated polymer chains probed by polarized single chromophore spectroscopy," *Appl. Phys. Lett.*, vol. 84, no. 7, p. 1183, 2004.

[29] M. N. Berberan-Santos and B. Valeur, "Fluorescence depolarization by electronic energy transfer in donor–acceptor pairs of like and unlike chromophores," *J. Chem. Phys.*, vol. 95, no. 11, p. 8048, 1991.

[30] A. a Bakulin, D. S. Martyanov, D. Y. Paraschuk, M. S. Pshenichnikov, and P. H. M. van Loosdrecht, "Ultrafast charge photogeneration dynamics in ground-state charge-transfer complexes based on conjugated polymers.," *J. Phys. Chem. B*, vol. 112, no. 44, pp. 13730–7, Nov. 2008.

[31] D. M. Basko and E. M. Conwell, "Theory of hot exciton dissociation in conjugated polymers," *Synth. Met.*, vol. 139, no. 3, pp. 819–821, Oct. 2003.

[32] V. Arkhipov, E. Emelianova, and H. Bässler, "Hot Exciton Dissociation in a Conjugated Polymer," *Phys. Rev. Lett.*, vol. 82, no. 6, pp. 1321–1324, Feb. 1999.

[33] K. Vandewal, S. Albrecht, E. T. Hoke, K. R. Graham, J. Widmer, J. D. Douglas, M. Schubert, W. R. Mateker, J. T. Bloking, G. F. Burkhard, A. Sellinger, J. M. J. Fréchet, A. Amassian, M. K. Riede, M. D. McGehee, D. Neher, and A. Salleo, "Efficient charge generation by relaxed charge-transfer states at organic interfaces.," *Nat. Mater.*, vol. 13, no. 1, pp. 63–8, Jan. 2014.

[34] J. Lee, K. Vandewal, S. R. Yost, M. E. Bahlke, L. Goris, M. a Baldo, J. V Manca, and T. Van Voorhis, "Charge transfer state versus hot exciton dissociation in polymer-fullerene blended solar cells.," *J. Am. Chem. Soc.*, vol. 132, no. 34, pp. 11878–80, Sep. 2010.

[35] A. E. Jailaubekov, A. P. Willard, J. R. Tritsch, W.-L. Chan, N. Sai, R. Gearba, L. G. Kaake, K. J. Williams, K. Leung, P. J. Rossky, and X.-Y. Zhu, "Hot charge-transfer excitons set the time limit for charge separation at donor/acceptor interfaces in organic photovoltaics.," *Nat. Mater.*, vol. 12, no. 1, pp. 66–73, Jan. 2013.

[36] J. F. Rubinson and Y. P. Kayinamura, "Charge transport in conducting polymers: insights from impedance spectroscopy.," *Chem. Soc. Rev.*, vol. 38, no. 12, pp. 3339–47, Dec. 2009.

[37] M. a. Loi, S. Toffanin, M. Muccini, M. Forster, U. Scherf, and M. Scharber, "Charge Transfer Excitons in Bulk Heterojunctions of a Polyfluorene Copolymer and a Fullerene Derivative," *Adv. Funct. Mater.*, vol. 17, no. 13, pp. 2111–2116, Sep. 2007.

[38] J. Bredas, J. Cornil, and A. J. Heeger, "The Exciton Binding Energy in Luminescent Conjugated Polymers **," *Adv. Mat.*, no. 5, pp. 447–452, 1996.

[39] E. Moore, B. Gherman, and D. Yaron, "Coulomb screening and exciton binding energies in conjugated polymers," vol. 106, no. October 1996, pp. 4216–4227, 1997.